

1 **Ready, set, go! An anticipatory action system against droughts**

2 Gabriela Guimarães Nobre^{1,*}, Jamie Towner¹, Bernardino Nhantumbo², Célio João da Conceição Marcos Matuele²,
3 Isaias Raiva², Massimiliano Pasqui³, Sara Quaresima³, Rogério Bonifácio¹

4
5 ¹ World Food Programme (WFP), Rome, Italy

6 ² Mozambique National Meteorology Institute (INAM)

7 ³ National Research Council, Institute for Bioeconomy, Rome, Italy

8
9 *Corresponding author: gabriela.nobre@wfp.org

10 11 12 **ABSTRACT**

13
14
15 The World Food Programme, in collaboration with the Mozambique National Meteorology Institute, is
16 partnering with several governmental and non-governmental organizations to establish an advanced early
17 warning system for droughts in pilot districts across Mozambique. The "Ready, Set & Go!" system is
18 operational in Mozambique for activating anticipatory action (AA) against droughts based on predefined
19 thresholds, triggers, and pre-allocated financing. The system uses bias corrected and downscaled seasonal
20 forecasts from the European Center for Medium-Range Weather Forecast (ECMWF) as core information
21 to anticipate severe reductions in rainfall during the rainy season. This information guides the
22 implementation of actions to reduce the impacts of rainfall deficits in the critical window between a
23 forecast and the onset of the drought event. Within this window of opportunity, the system releases an
24 alert for readiness (Ready) and activation (Set) preceding the mobilization of anticipatory action on the
25 ground (Go). With the recent adoption of the Southern African Development Community Maputo
26 Declaration on *Bridging the Gap between Early Warning and Early Action*, member states have committed
27 to enhancing the reach of early warning system by leaving no one behind. Therefore, there is a need to
28 assess the opportunities and limitations of the Ready, Set & Go! system to scale up drought AA
29 information to all districts in Mozambique. This study describes the Ready, Set & Go! system which uses
30 ensemble forecasts of the Standardized Precipitation Index to trigger anticipatory action against droughts
31 on a seasonal timescale. The Ready, Set & Go! optimizes the use of seasonal forecast information by
32 choosing triggers for anticipatory action based on verification statistics and on a double confirmatory
33 process, which combines longer lead times with shorter lead time forecasts for issuing drought alerts. In
34 this study, we show the strengths of the system by benchmarking it against three simpler triggering
35 approaches. Our findings indicate that the Ready, Set & Go! system has significant potential to scale up
36 AA activities against severe droughts throughout the entire rainy season, covering on average 76% of the
37 Mozambican districts. This approach outperforms the three benchmarked methods, demonstrating
38 higher hit rates, extended lead times, and a lower false alarm. If efforts are concentrated on the first part
39 of the rainy season, national coverage against severe droughts could be expanded to 87% of all districts.
40 By aligning with the objectives outlined in the Maputo Declaration and the Early Warning for All initiative,
41 this research contributes to safeguarding communities against the adverse impacts of climate-related
42 events, aligning with the ambitious goal of universal protection by 2027.

45 1. INTRODUCTION

46 Mozambique experienced in 2015/16 one of its worst drought events in decades, which affected the food
47 security of approximately 2.3 million people leading to its government to declare a state of national
48 emergency (OCHA, 2017). This El Niño induced drought caused an exceptional lack of precipitation in two
49 consecutive rainy seasons, which resulted in significant losses in rain-fed yields, below-average irrigated
50 crops, poor pasture conditions and high cattle mortalities (WFP, 2016). The dryness propagated into water
51 reservoirs in southern Mozambique, where the impact on water levels remained for five years (ECHO,
52 2021).

53
54 Mozambique is a country exposed and vulnerable to multiple hazards due to its geographical location and
55 latitudinal extent. Its climate is affected by several modes of climate variability such as the El Niño-
56 Southern Oscillation (ENSO; Rapolaki et al., 2019; Blamey et al., 2018), Indian Ocean Dipole (IOD; Ashok
57 et al., 2001; Manatsa et al., 2011; Saji et al., 1999) and the Subtropical Indian Ocean Dipole (SIOD; (Behera
58 & Yamagata, 2001). These climate modes of variability modulate the frequency and intensity of the
59 various weather systems that are directly associated to multiple natural hazards happening as a single or
60 consecutive risk (e.g., Hart et al., 2010; A. J. Manhique et al., 2015; Atanásio João Manhique et al., 2021;
61 Mawren et al., 2020; Rapolaki et al., 2019; Reason & Keibel, 2004). Impacts of single and consecutive
62 hazards including flooding, cyclones and droughts are exacerbated by poverty and weak institutional
63 development, where climate related disasters are one of the main driving forces of inequalities and food
64 insecurity in the country (Baez et al., 2019; De Ruiter et al., 2020). In Mozambique, nearly 25% of its
65 population live in areas with a high probability of experiencing a climate shock (World Bank, 2018).
66 Therefore, the adoption of protective mechanisms and systems to anticipate and prepare the government
67 and communities to climate shocks is crucial for building resilience and sustainable development.
68 Recently, the national government has made climate risk management a priority strategy following the
69 adoption of the Maputo Declaration *on Bridging the Gap between Early Warning and Early Action*, in
70 which member states of the Southern African Development Community (SADC) have committed to take
71 an active people-centered role to ensure all citizens access to effective Early Warning and Early Action
72 systems (SADC, 2022).

73
74 Since 2019, a multi-sector government-led anticipatory action (AA) trigger system against drought (WFP,
75 2023b) has been under development in Mozambique coordinated by the Mozambique National Institute
76 of Disaster Management (INGD) with the technical support of relevant actors, including the National
77 Meteorological Institute (INAM) and the World Food Programme (WFP). Droughts are a slow, recurrent,
78 and predictable phenomena (Guimarães Nobre et al., 2023) and yet, they cause an estimated yearly loss
79 of US\$20 million (Baez et al., 2019) to Mozambique. Drought early warning system (EWS) have a great
80 potential to reduce some of these losses when AA is implemented ahead of a shock based on forecast
81 information. Previous studies have assessed the skill of seasonal forecasts to predict the onset of droughts
82 (Gebrechorkos et al., 2022; Guimarães Nobre et al., 2023; Trambauer et al., 2015; Winsemius et al., 2014)
83 whereas only few have focused on an in depth interpretability of the forecast quality through the lenses
84 of decision-making and practical implications. For instance, a reflection on the adequateness of lead time

85 of information for action, and/or definition of probabilistic trigger values for releasing drought alerts and
86 advisories for AA are aspects largely missing in the scientific literature.

87

88 AA approaches are gaining more traction with an increased number of institutions dedicating funding and
89 pilot studies in Mozambique and elsewhere. There are currently anticipatory action initiatives and
90 projects in 43 countries, supported by 179 organizations, including the Red Cross movement and UN
91 entities such as the United Nations Office for the Coordination of Humanitarian Affairs and WFP
92 (Anticipation Hub, 2024). However, the evidence on the benefits of acting earlier is still fairly new and
93 limited. Overall, existing evidence based on pilot experiences in other parts of the world have mainly
94 suggested a positive impact of AA at household level, with beneficiaries reporting higher crop productivity
95 and less food insecurity during prolonged periods of drought (Weingärtner et al., 2020). In Mozambique,
96 AA drought pilots are limited - to date - to eleven districts and further scale up of activities to the national
97 level is desired. However, an assessment of the opportunities and limitations of the current drought AA
98 trigger system is currently missing, especially given the 2023 El Niño scenario, which is expected to
99 negatively affect the 2023-24 rainy season. In response to the need of assessing the potential to bring AA
100 to scale, this study describes the operational triggering system for drought AA being piloted in
101 Mozambique during the southern Africa rainy season 2023-24. This article presents the analytical routines
102 involved in the definition and monitoring of triggers for AA as describes the technical methodologies of
103 the system by outlining data processes, forecast application, decision-making and operational activities
104 linked to the release of AA advisories to pilot areas.

105

106

107 2. CASE STUDY & METHODS

108 2.1 Case Study

109 We developed a methodology that is being piloted and scalable for triggering AA against droughts for all
110 districts in Zimbabwe and Mozambique, although this study has a special focus on the latter. Currently in
111 Mozambique, a government-led AA plan is in place for 11 pilot districts (see Figure 1). However, an
112 anticipatory action system is desired for the whole country requiring the upscaling of the current set up.
113 Concerning climatology, the rainy season in Mozambique lasts from October to May, although the largest
114 amounts are experienced between November and April. The wettest months are December and January,
115 however January alone is the wettest month across the country (WFP, 2018). Rainfall amounts increase
116 from south to north. For instance, areas of low annual rainfall (less than 500 mm) include the southern
117 provinces of Maputo, Gaza, Inhambane and the southern half of Tete, whereas areas of high total rainfall
118 (over 2000 mm) include the provinces of Cabo Delgado, Niassa, Nampula and Zambezia. Rainfall
119 interannual variability is stronger in areas of lower rainfall totals and is a major limiting factor to
120 livelihoods and small-scale rain-fed agriculture (Guimarães Nobre et al., 2023). In addition, the province
121 of Gaza has a remarkably variable and short growing season length (mostly below 3 months). Interannual
122 climate variability in the southern Africa region is particularly linked to the El Niño-Southern Oscillation
123 (ENSO) (Richard et al., 2001). During the months of October to December, the El Niño phase often drives
124 rainfall increases (decreases) in Cabo Delgado and Niassa in northern Mozambique (southern provinces
125 of Maputo, Gaza and Inhambane). During these months, when a La Niña state is observed, rainfall
126 increases are observed in parts of the central provinces of Manica, Sofala and northern Inhambane. In
127 addition, during the months of January to March, El Niño leads to drier conditions across most of the
128 country, whereas in the south and centre of the country a moderate increase in rainfall is observed during
129 La Niña phases (WFP, 2018). Mozambique is highly climate vulnerable country where livelihoods rely on
130 local natural resources (e.g., agriculture and fisheries) as their primary economic activity. Drought events
131 affect the ability of farmers and fishermen to sustain crops and fish, often cascading into situations of
132 food insecurity, malnutrition, and unsustainable incomes.

133

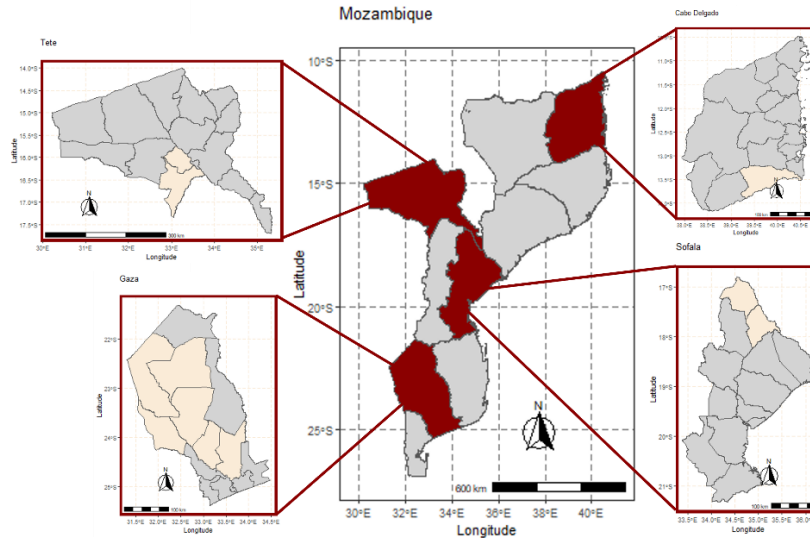


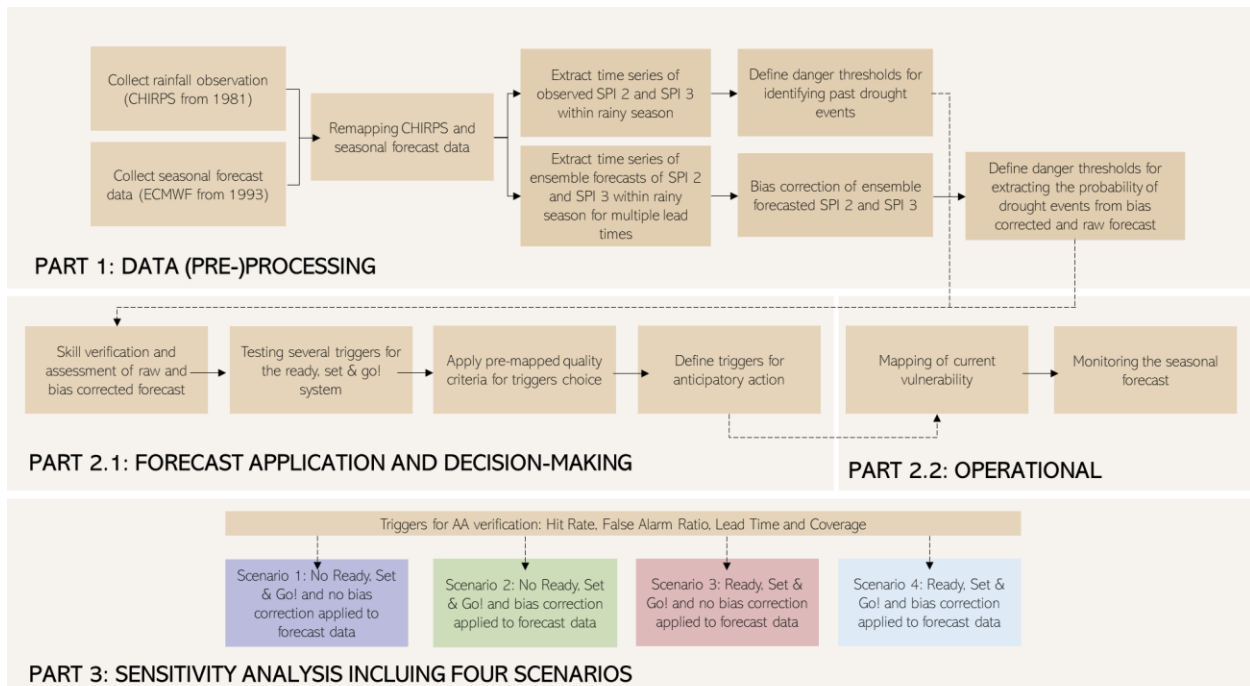
Figure 1: Districts in Mozambique with government-approved anticipatory action plans.

134
135

136 2.2 Methodological Framework

137 The operational triggering system for drought AA is developed and tested in three stages (Figure 2): (1)
138 data pre-processing, (2) forecast application and decision-making, and (3) sensitivity analysis. A detailed
139 explanation of each stage is provided in sections 2.2.1 to 2.2.3.

140
141



142
143
144

Figure 2: Flowchart of the methodological framework applied in this study, handled in three stages: (1) data pre-processing; (2) forecast application and decision-making; and (3) sensitivity analysis.

145 2.2.1 Part 1: Data pre-processing

146 **Collect rainfall observation (from 1981)**

147 As source of rainfall estimates, we use daily blended precipitation records from the Climate Hazards group
148 Infrared Precipitation with Stations version 2 (CHIRPS) for the period of January 1981 to near present.
149 CHIRPS is a high resolution (0.05°) precipitation dataset, which is used for drought early warning purposes
150 by the Famine Early Warning Systems Network This dataset integrates data from real-time meteorological
151 stations with infrared satellite data (therefore called blended precipitation product), covering from 50°N
152 to 50°S via a blending procedure further described in Funk et al. (2015).

153

154 **Collect seasonal forecast data (ECMWF from 1993)**

155 As source of forecast data, we use seasonal precipitation forecasts from the ECMWF's seasonal forecasting
156 system (SEAS5) for the period 1993–2022. In its native resolution, the forecast is available at 1 arc-degree
157 and new forecasts are released monthly on the fifth day covering the coming 7 months. SEAS5 is
158 composed of a set of 25 ensemble members until 2016 (hindcast period), and 51 ensemble members from
159 2017 onwards as part of the operational system (Ratri et al., 2019). It is important to highlight that ECMWF
160 SEAS5 has a new version (SEAS5.1) since November 2022 with extended hindcast until 1981 which full
161 time series of hindcast and operation forecast can be freely downloaded from the Copernicus Climate
162 Data Store.

163 **Remapping CHIRPS and seasonal forecast data**

164 Since the datasets of rainfall estimates and forecasts are available in different spatial resolutions, we
165 remapped them into an intermediate resolution of 0.25°. This moderate resolution was chosen taking into
166 consideration the size of pilot districts in which the system will be implemented, computational capacity
167 as well as to reduce the impact of rainfall small-scale variability. For this process, we used bilinear
168 interpolation one of the most commonly used methods of climate grid interpolation (National Center for
169 Atmospheric Research Staff, 2014). Bilinear interpolation resizes the data by estimating values at a point
170 by averaging the values of the surrounding points.

171

172 **Extract time series of observed SPI 2 and SPI 3 within rainy season**

173 From the daily CHIRPS rainfall estimates, we extract the Standard Precipitation Index (SPI), a widely used
174 indicator for measuring rainfall variability over a long-term climatological period (Svoboda et al., 2012).
175 The SPI is centered around the mean rainfall for a given time and location, with values ranging from -4 to
176 +4. Negative SPI values indicate various levels of rainfall deficits, which are particularly relevant to the
177 designed trigger system. The SPI can also highlight drought situations when a “danger threshold” is
178 identified signaling rainfall deficits severe enough to prompt anticipatory to mitigate the impacts on
179 livelihoods.

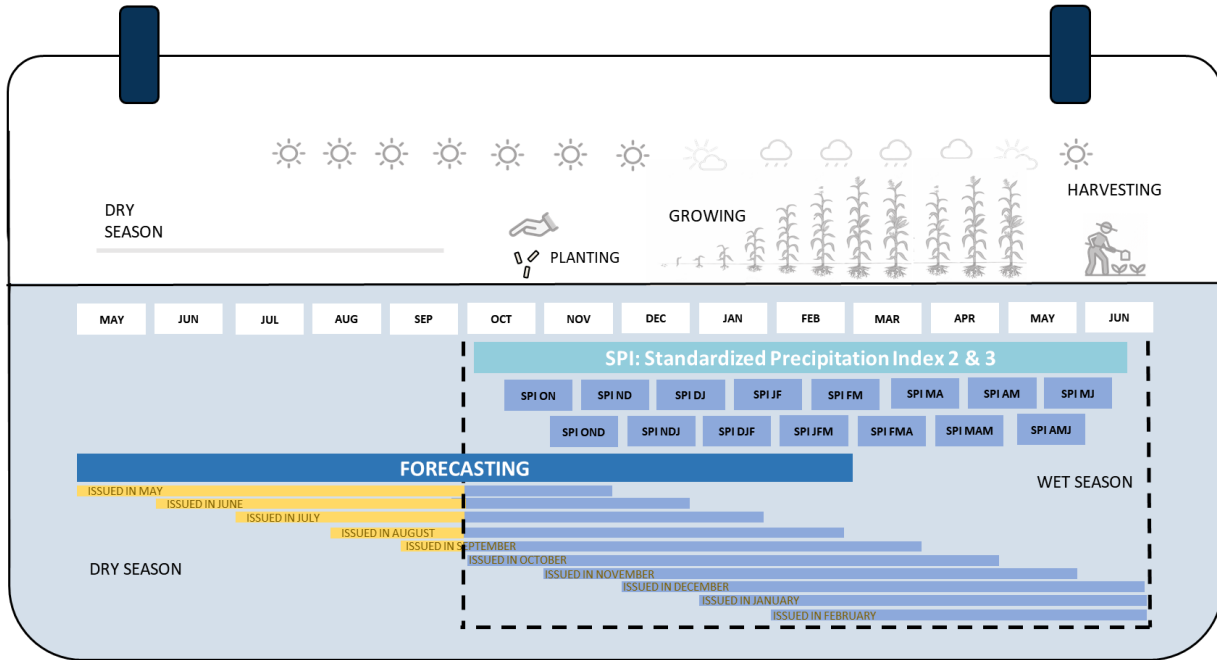
180

181 In this study, SPI values are calculated using two- and three-month accumulation periods (SPI 2 and SPI 3,
182 respectively). These accumulation windows are particularly suitable for detecting risks to agricultural
183 systems during the crop development cycle. It is crucial to note that the AA framework aims to protect
184 food security by reducing the risk of crop failures in rain-fed systems. Therefore, only SPI values extracted
185 during the rainy season are relevant to the trigger system (see the section below for a detailed explanation
186 of windows of opportunity for anticipatory action).

187
188 To derive the SPI estimates, the CHIRPS rainfall dataset, accumulated over two and three months, is fitted
189 to a gamma distribution and subsequently transformed to a normal distribution with z-values (Lloyd-
190 Hughes & Saunders, 2002). The period from 1981 to 2018 serves as the reference climatology for
191 calculating the gamma distribution parameters. This period was selected due to the availability of a
192 complete series of rainfall observations at the start of the project in 2019. Periods with zero precipitation
193 are handled by assigning SPI values based on the historical occurrence of such periods from 1981 to 2018.
194 However, since we use precipitation data accumulated over two and three months, zero values are rare,
195 especially as SPI is only extracted during the rainy season. For extracting SPI during the dry season or in
196 arid regions, more sophisticated techniques, such as those described by Stagge et al., (2015) are available
197 and should be preferred.

198 **Extract time series of ensemble SPI 2 and SPI 3 within rainy season for multiple lead times**

199 For the forecasting series, the parameters of the gamma distribution are determined using data from all
200 ensemble members for the years 1993 to 2018, as data prior to 1993 is not available in the Copernicus
201 Climate Data Store (SEAS5). The routine adopted for handling zero values is similar to the one described
202 for deriving SPI estimates (see above). In Figure 3, we illustrate the extraction of SPIs for various lead times
203 of the forecast system with a seven-month lead time. For example, the seasonal forecast released at the
204 beginning of May covers the subsequent months (May to November). Therefore, the only indicator
205 extracted from this forecast is SPI 2 ON, as October marks the first month of the rainy season in the
206 country.



208
209
210

Figure 3: Illustration of the SPIs representing rainfall anomalies during Mozambique's rainy season, along with the corresponding forecast months used for their extraction.

211

Define danger threshold for identifying past drought events

212

213 Given that the Standardized Precipitation Index (SPI) is linked to the probability of certain rainfall amounts,
214 we convert a specific z-value into an expected frequency by calculating the area under the normal
215 distribution curve up to that z-value. This proportion, or probability (p), is then converted into a return
216 period (T) by taking the inverse of the probability ($p = 1/T$). In the operational AA trigger system, three z-
217 value thresholds are used, as highlighted by Guimarães Nobre et al (2023), corresponding to different
218 severity levels. This article focuses on the most severe category in the AA trigger system, which is $SPI \leq -1$
219 as this negative anomaly is expected to cause the most significant damage among those adopted by the
220 system.

221

222 However, it is important to highlight that the impact of a drought threshold should ideally be estimated
223 using historical observations combined with information on who and what is exposed to a hazard
224 (exposure and vulnerability). Due to the lack of extensive drought impact data at the district level, the
225 choice of a threshold level is based on frequencies suitable for AA operations in the region. Typically, AA
226 programs target hazards that occur at least once every three to six years on average. Implementing AA
227 pilots periodically is crucial for enhancing program activities. Consequently, thresholds for AA operations
228 should not be set too low, given that the occurrence of drought events of such intense magnitude is rare.
229 A $SPI \leq -1$ (named severe category in the AA trigger system) corresponds to an event occurring
230 approximately once every 6 to 7 years (or $p = 15.87\%$). By applying the $SPI \leq -1$ threshold to the SPI2 and

231 SPI3 estimated series, we obtain a time series since 1981 of past drought events for the respective two-
232 and three-month periods in the pilot districts.

233

234 **Bias correction of ensemble forecasted SPI 2 and SPI 3**

235 We employ a quantile-quantile mapping technique, conditioned on the state of ENSO, to adjust SPI
236 forecast values. This is achieved by aligning the cumulative density function of SPI forecasts at each grid
237 cell with the reference SPI data extracted from CHIRPS at the corresponding grid cell and its k nearest
238 neighbors. The SPI forecast and reference distributions are matched by establishing an ENSO-informed,
239 quantile-dependent correction function. This function adjusts the forecast quantiles based on their
240 observed SPI counterparts, translating the SPI forecast time series into bias-adjusted values that
241 accurately represent the observed SPI data distribution.

242

243 The transfer functions for bias correction are developed based on the SPI reference and SPI forecast time
244 series, specifically targeting the AA drought indicator rather than daily or monthly rainfall. By
245 incorporating ENSO information, we aim to ensure that rainfall variability is more accurately represented
246 in the corrected forecast data, especially in regions and timescales where ENSO has a significant impact
247 (Manzanas & Gutiérrez, 2019). This approach combines statistical quantile mapping bias correction with
248 ENSO state knowledge during rainy seasons. Furthermore, information from the nearest neighbors from
249 the reference pixel is used to account for the spatial dependence inherent in climate data (k=9) (Cannon,
250 2018) and to extend the SPI time series used to create the transfer function. By targeting the SPI indicator
251 directly with the transfer function, we aim at increasing the accuracy of drought detection by bringing SPI
252 forecasts closer to the observed SPI climatology, ensuring that the SPI derived from forecasts are more
253 consistent with historical patterns and trends. This is critical for the Ready, Set and Go! System that
254 releases alerts based on negative anomalies through the SPI indicator rather than on rainfall amounts.

255

256 In practical terms, incorporating ENSO information into quantile mapping involves: (i) categorizing data
257 by ENSO phases; (ii) generate empirical cumulative distribution functions for each ENSO phase separately
258 for both SPI observed and SPI forecast; (iii) perform quantile mapping by applying the transfer function to
259 the test year (year left out during cross validation) of the analysis according to the ENSO phase of the year
260 being bias corrected; iv) combine corrected forecast outputs if bias correction is found to improve skill in
261 detecting droughts.

262

263 In summary, the quantile mapping transfer function corrects the SPI forecast based on the SPI reference
264 value of the pixel under investigation and its nine neighboring pixels conditioned on the state of ENSO. To
265 prevent inflating the skill of the bias correction, a leave-one-year-out cross-validation (LOCV) scheme is
266 used. The bias correction transfer function is constructed by pooling all ensemble members of the forecast
267 and then applied to all members of the left-out test year.

268

269 An overview of this scheme is available in Figure 4. For a list of ENSO years, see Supplementary Material
270 S1.

271

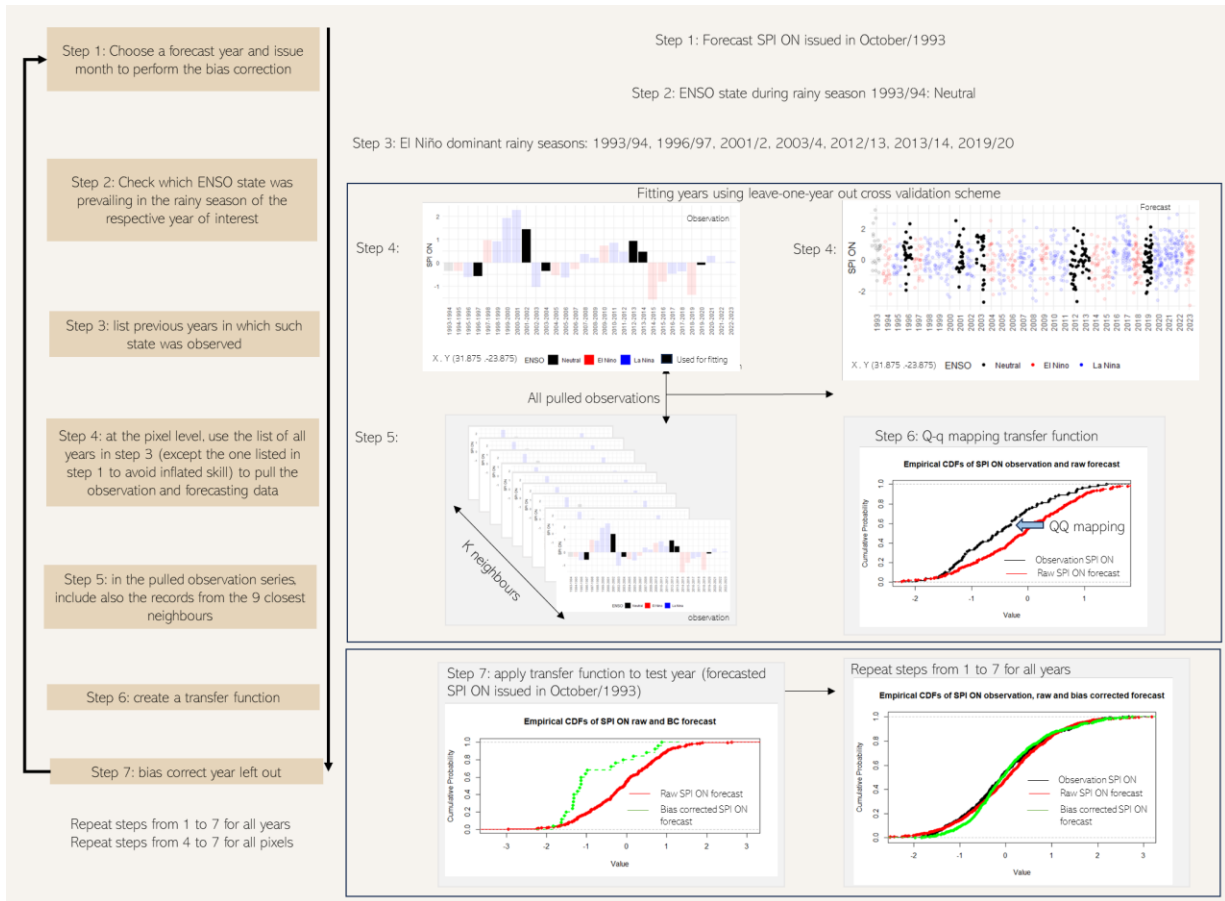


Figure 4: Bias correction methodology in seven steps next to an illustrative example.

273
274

275

276 **Define danger threshold for extracting the probability of drought events from bias corrected and raw**
277 **forecasts**

278 From both raw and bias-corrected forecasts, we apply the danger threshold ($SPI \leq -1$, classified as severe
279 in the AA trigger system) to determine the probability of a severe drought. This is done by calculating the
280 proportion of ensemble members that meet or fall below the threshold. We repeat this process for each
281 forecast issue month from 1993 to 2022, creating a time series of drought probabilities at different lead
282 times for both the raw and bias-corrected forecasts.

283

284 In practice, the bias-corrected drought probabilities replace those from the raw forecast only when there
285 is a demonstrable gain in skill for forecasting severe drought. This gain in skill is evaluated by comparing
286 the area under the Receiver Operating Characteristic (AUROC) curve scores of the raw and bias-corrected
287 forecasts (further detailed in the section below). Consequently, the bias-corrected drought probability
288 information is used only if it shows an improved ability to predict severe droughts in the pilot districts,
289 considering specific cases (such as a particular forecasts lead time and SPI 2 and SPI 3 aggregation).

290 2.2.2 Part 2.1: Forecast application and decision-making

291 **Skill verification and assessment of raw and bias corrected data**

292 As described in the previous section, we obtain drought probabilities from both the raw and bias-
293 corrected forecasts. For each specific district, lead time, and SPI indicator, we use the forecast with the
294 higher skill in predicting severe drought to develop triggers for the AA. The forecast with lower skill is
295 discarded from the AA system. Skill is assessed by extracting and comparing the AUROC scores of the
296 forecasts.

297
298 The AUROC score (e.g., Fawcett, 2006) is a widely applied indicator that measures the ability of a
299 probabilistic forecast to discriminate between a binary outcome (e.g., severe drought or no drought). The
300 AUROC score calculation requires setting a range of trigger values to convert a probability forecast into
301 categorical, and therefore is related to decision-making in response to whether the forecast should
302 release an alert. For the releasing of a “drought alert”, several triggers are tested, and a graph (known as
303 a ROC curve) is produced to summarize the hit rate and false alarm rate that can be expected from
304 different probability trigger values. The area under the ROC provides a summary statistic for the
305 performance of probability forecasts, ranging from 0 to 1 (worst to best). Forecasts with little or no skill
306 have a ROC score of approximately 0.5. Forecast is perfectly incorrect when the ROC is zero. In summary,
307 for a specific district, lead time and SPI indicator, we choose which source of forecast to use for the Ready,
308 Set & Go! triggers (raw or bias corrected) based on the forecast skill assessment informed by the AUROC
309 score at the district level.

310

311 **Testing several triggers for the for the Ready, Set & Go! system**

312 Triggers for anticipatory action indicate the forecasted severity of drought that would prompt a response.
313 If the forecast exceeds the trigger, funds are automatically allocated, and anticipatory actions are
314 initiated. A trigger is essentially a value that converts a probability forecast into a decision on whether to
315 take action, effectively determining whether a drought alert should be issued. Defining a trigger involves
316 understanding when forecasting information can be trusted to successfully mobilize anticipatory actions,
317 despite inherent uncertainties. Therefore, triggers are based on the skill levels of the forecasts, requiring
318 an investigation of past forecast accuracy and an acknowledgment of forecast uncertainty.

319
320 Forecasts at any lead time can be tested to derive triggers for anticipatory action. It is common practice
321 for organizations to define two types of triggers for anticipatory action: (i) a preparedness trigger with a
322 longer lead time and (ii) a confirmatory trigger for the activation of activities with a shorter lead time
323 before the drought onset. These triggers are defined based on the skill levels of the forecasts for each lead
324 time. However, testing lead times independently may result in an unrealistic performance of the
325 anticipatory action program, as the system relies on both triggers being exceeded, even though they are
326 set based on their individual performance. Additionally, organizations may assign preparedness and
327 activation activities based on a single trigger from a specific lead time. This approach can vary depending
328 on the organization's specific capacity to respond to the forecasted information.

329

330 The Ready, Set, & Go! system employs a double confirmatory approach for drought alerts. This means
331 that the trigger value, tailored for each forecast month, district, and SPI indicator, must be exceeded for
332 two consecutive months to prompt action. The performance of these triggers for anticipatory action is
333 evaluated in combination rather than individually. For example, if the trigger based on the August forecast
334 for Chibuto district, which predicts potential severe droughts in October-November, is exceeded, the
335 "ready" phase is activated. If the trigger based on the September forecast for the same district is also
336 exceeded, the "set" phase is activated, and activities are immediately mobilized on the ground, initiating
337 the "Go!" phase. Testing triggers in combination with a double confirmation process aims to create a more
338 accurate trigger system and provide a longer window for readiness and preparedness activities before AA
339 implementation. This approach is validated using a sensitivity analysis explained in section 2.2.4.

340
341 For instance, readiness activities might involve preparing internal documents, which can then lead to
342 initiating a procurement process if an AA advisory is issued. Practically, for each forecast month that can
343 produce a "ready" and "set" trigger, we jointly test several candidate pairs of triggers. This testing is
344 conducted in steps of 1% ranging from 0% to 100%, resulting in 10,201 combinations of candidate triggers.
345 This is done for each district, pair of forecast months, and SPI 2/SPI 3 indicator. For a complete overview
346 of the triggers for SPI ON for a given district, we test all candidate pairs of triggers for the following forecast
347 month combinations: May (ready) and June (set), June (ready) and July (set), July (ready) and August (set),
348 August (ready) and September (set), and September (ready) and October (set). For each pair of triggers,
349 we calculate key performance metrics (e.g., hit rate and false alarm ratio) to evaluate how the drought
350 alerts would have performed in the past. The relevance of these metrics was identified during a workshop
351 held in 2022 with governmental partners.

352
353 **Apply pre-mapped quality criteria for the triggers' choice**
354 The definition of a trigger value for drought AA is intrinsically linked to the skill of the forecast and the
355 identification of a certain degree of risk tolerance levels by users of the forecast (Lopez et al., 2018). In
356 practice, when a low probability trigger value is chosen, one can expect to forecast droughts frequently,
357 whereas if a very high value is chosen, the opposite is expected to happen. The optimum trigger value
358 should reflect appropriateness through the lenses of the decision-maker and the relative importance
359 given to drought false alarms versus missed drought events.

360
361 Users who are averse to missing a drought, will choose a lower trigger value and deal with an increase in
362 false alarms. For instance, a low trigger value can be a suitable option for actors that seek to assist very
363 fragile populations and/or when the portfolio of AA is considered "non-regret" (Chaves-Gonzalez et al.,
364 2022). Anticipatory actions are classified as "non-regret" when they are worth investing in even if a crisis
365 does not materialize and would not be regretted with hindsight. Following this approach, we have created
366 a menu of "emergency triggers", to be used when pilot districts are experiencing high levels of
367 vulnerability. On the other hand, users who are averse to false alarms will choose a higher trigger and
368 manage occasional missed events. For instance, a high trigger value can be a suitable option for actors
369 that have limited funds and/or when the portfolio of AA contains actions that affect livelihoods, such as
370 evacuations, which are considered highly regrettable if a false alarm occurs. This approach can be of high
371 relevance for scaling up AA to all districts in Mozambique as the largest geographical coverage is desired

372 and funding distribution/sharing across a wide area is expected. Following this approach, we have created
 373 a menu of "general triggers", to be used when pilot areas are experiencing normal to low levels of
 374 vulnerability. As displayed in Table 1, the expected performance of both menus is different, especially
 375 concerning the tolerance to false alarms and the probability of drought detection. Operationally, the
 376 assessment of vulnerability information is done prior to the start of AA season in Mozambique (more
 377 explanation in section 2.2.3).

378
 379 Table 1: List of quality criteria for assigning forecast-based triggers for severe drought events. It is important to highlight that criterion
 380 5 plays a role in the calculation of criteria 2, 3 and 4.

Number	Criteria for determining triggers	General menu	Emergency Menu
1	The selected trigger must have predicted at least (x%) of the past droughts	55	70
2	The chance of successfully implementing AA following a ready & set alert must be greater than (x%)	65	55
3	The chance of unsuccessfully implementing AA following a ready & set alert must be less than (x%)	35	45
4	Return period (years) for the implementation of AA against droughts	7	6
5	Actions will only be counted as "in vain" if the ready & set alert for severe drought is followed by an SPI of:	SPI > -0.68	
6	Minimum number of full months for the Go! Phase (implementation)	1	

381
 382 **Define triggers for anticipatory action**
 383 After testing all combinations of trigger pairs for the "ready" and "set" phases and recording the statistics
 384 listed in Table 1, we began a selection process based on the quality criteria outlined in the same table.
 385 The suitable pairs were ranked according to their hit rate and false alarm ratio, considering both district-
 386 specific performance and the stage of the rainy season: (i) start to mid-season (referred to as Window 1)
 387 and (ii) mid- to end of season (referred to as Window 2). Only the best-performing trigger pairs were
 388 selected for further analysis, which is presented in the results section 3.4.

389
 390 It is important to clarify that AA targets these two windows of the rainy season because the activities
 391 implemented before the onset of drought within these periods serve different purposes. The forecast of
 392 drought risks within these windows informs the refinement of the AA portfolio, as rainfall deficits during
 393 the start to mid-season and mid- to end-season are expected to impact crops differently. For example, AA
 394 implemented before potential droughts in Window 1 aims to support planting and sowing activities, such
 395 as distributing drought-tolerant seeds, while AA implemented in Window 2 focuses on supporting
 396 livelihoods, such as providing cash transfers.

397
 398 Furthermore, due to the variation in climatology across the country, the periods covered by Windows 1
 399 and 2 differ by zone, shifting by approximately one month from south to north. Table 2 provides an

400 overview of the timing of these windows, the indicators used to assess drought risks within them, and the
 401 provinces associated with each zone. The division of the rainy season into these windows was defined by
 402 the Technical Working Group (TWG) for drought early warning systems (EWS) and AA, which includes
 403 several governmental and non-governmental institutions (WFP, 2023). Further details can be found in the
 404 discussion section.

405
 406 Table 2: Description of anticipatory action windows per zone and province with an illustration of SPI indicators informing drought
 407 events.

Zone	Provinces	Months within window 1	SPI 2 and SPI 3 informing window 1	Months within window 2	SPI 2 and SPI 3 informing window 2
North	Nampula, Cabo Delgado and Niassa	December to March	SPI DJ, SPI DJF, SPI JF, SPI JFM, SPI FM	March to June	SPI FMA, SPI MA, SPI MAM, SPI AM, SPI AMJ, SPI MJ
Central	Manica, Sofala, Tete and Zambezia	November to February	SPI ND, SPI NDJ, SPI DJ, SPI DJF, SPI JF	February to May	SPI JFM, SPI FM, SPI FMA, SPI MA, SPI MAM, SPI AM
South	Gaza, Inhambane, Maputo City and Maputo	October to January	SPI ON, SPI OND, SPI ND, SPI NDJ, SPI DJ	January to April	SPI DJF, SPI JF, SPI JFM, SPI FM, SPI FMA, SPI MA

408
 409 2.2.3 Operational

410 Once the repository of triggers for AA has been finalized, several operational activities follow. Although
 411 these activities do not impact the overall system performance (as presented in the results section), they
 412 provide valuable insight into the operationalization of the methodology showcased in this study. The first
 413 key activity following the initiation of forecast and trigger monitoring for AA is a vulnerability analysis. This
 414 analysis is conducted annually, typically around April and May as the rainy season concludes. Its purpose
 415 is to assess the levels of vulnerability in the AA pilot districts by examining recent climate shocks and
 416 projected food security outcomes. The results of this analysis inform decisions about which set of
 417 triggers—general or emergency—each pilot district should employ for the upcoming AA season. For
 418 example, if a district experienced drought during the most recent rainy season, with anticipated negative
 419 impacts on food security, the emergency triggers are selected for the next AA season due to the
 420 heightened vulnerability in that area. Once this decision is made, forecasts from May to February of the
 421 following year are processed, and the AA triggers are monitored on a monthly basis. The monitoring of
 422 the Ready, Set, & Go! system triggers is conducted by INAM and WFP, with updates communicated to the
 423 Technical Working Group (TWG) for drought early warning systems (EWS) and AA through a dashboard
 424 and regular bulletins.

425 2.2.4 Sensitivity analysis including four scenarios

426 We evaluate the robustness of our methods through a sensitivity analysis, considering four distinct
 427 scenarios. For each scenario, we extract four key metrics:

- 428 1. **Hit Rate:** percentage of past severe droughts accurately captured by the AA trigger(s).

- 429 2. **Tolerant False Alarm Ratio:** This metric accounts for false alarms when the AA trigger is exceeded,
430 but the drought threshold is narrowly missed. For example, a false alarm occurs if a severe
431 drought trigger ($SPI \leq -1$) is followed by an SPI value just below the threshold (e.g., -0.99). To better
432 contextualize false alarms, we calculate "tolerant" false alarm ratio, which considers the number
433 of severe drought alarms followed by an SPI greater than -0.68 (see Table 1) introduces extra
434 tolerance when analyzing forecasting errors, as severe drought alerts followed by SPI values
435 between -0.68 and -0.99 are not counted as non-drought situations. This approach is based on
436 the practical assumption that AA interventions will still benefit the population, even if
437 implemented during a slightly less severe dryness.
- 438 3. **Lead time of implementation:** the time difference between the starting month of the SPI indicator
439 and the month in which the forecast was issued. For instance, a forecast issued in May is
440 considered to have a lead time of 4 months when providing outlooks of SPI ON.
- 441 4. **AA percentage coverage:** percentage of Mozambican districts where an AA trigger was identified,
442 meeting the criteria outlined in Table 1.

443

444 It is important to clarify that these metrics were derived from the skill assessment of the forecasts from
445 1993 to 2021. Specifically, the number of hits and false alarms during this period is used to calculate a key
446 metric from the quality criteria list: the "Return Period (Years) for the Implementation of AA Against
447 Droughts." This metric helps determine whether the empirical frequency of AA interventions aligns with
448 the frequency of the threshold for severe droughts. Furthermore, the scenarios for the sensitivity analysis
449 are defined as follows:

450

- 451 1. Scenario 1: An AA advisory based solely on a single alert, using only one lead time from the raw
452 SPI forecasts.
- 453 2. Scenario 2: An AA advisory based solely on a single alert, using either raw or bias-corrected SPI
454 forecasts, depending on which has the highest skill.
- 455 3. Scenario 3: An AA advisory requiring double confirmation but using only raw SPI forecasts.
- 456 4. Scenario 4: An AA advisory based on the Ready, Set, & Go! system, requiring double confirmation
457 and using a combination of bias-corrected and raw SPI forecasts.

458 3. RESULTS

459 3.1 Zonal based overview of the years with severe drought conditions within the rainy season

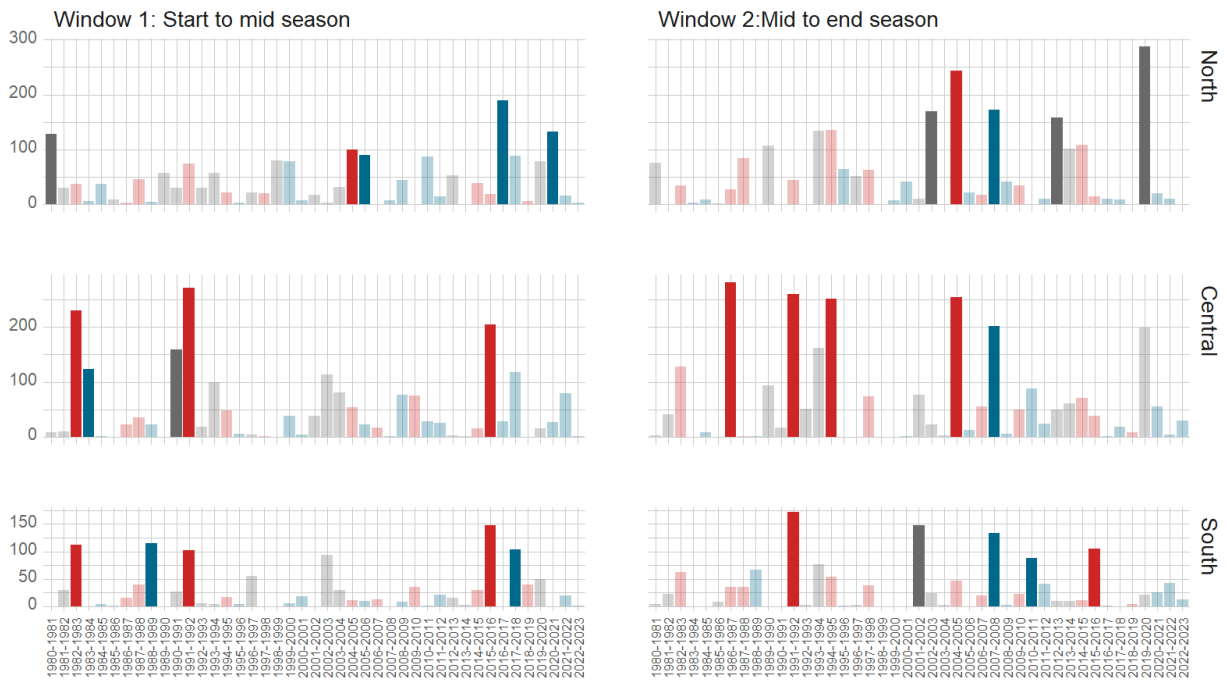
460 In Figure 5, we illustrate the frequency of severe drought occurrences during the rainy season from 1981
461 to the present. We began by extracting the mean SPI 2 and SPI 3 indicators for each district, focusing on
462 the rainy windows relevant to each district/province (see Table 2 for SPI indicators and their associated
463 windows). We then counted how often the severe drought threshold was met or exceeded. The top 5
464 years with the highest number of 2- and 3-month periods experiencing severe drought conditions are
465 highlighted. Bars in the figure are colored to indicate the ENSO phase during the respective rainy seasons
466 in Mozambique (see Supplementary Material S1 for classification). To simplify the data presentation,

467 districts are grouped by zones (refer to Table 2 for zone-to-province list). A similar overview of severe
 468 drought years at the province and district levels is provided in Supplementary Material S2.

469
 470 Overall, severe drought conditions can occur during any of the three ENSO phases across all zones. This
 471 underscores the need for an AA system that is effective regardless of the ENSO phase. However, we found
 472 that severe droughts are significantly more frequent during El Niño phases (mean frequency = 66)
 473 compared to Neutral (mean frequency = 41) and La Niña phases (mean frequency = 31), as confirmed by
 474 a t-test ($p < .01$). Previous studies also support this finding (Araneda-Cabrera et al., 2021; Lyon & Mason,
 475 2007). Additionally, the top 5 drought years for different windows vary considerably. In the North zone,
 476 only the rainy season of 2004-05 appears in the top 5 for both windows. In the Central zone, only the
 477 1991-92 rainy season ranks in the top 5 for both windows. In the South zone, the rainy seasons of 1991-
 478 92 and 2015-16 are among the top 5 for both windows. This variation highlights the importance of
 479 developing an early warning system that accounts for different intra-seasonal rainfall patterns and adjusts
 480 operations according to the stages of the rainy cycle.

481

**Count of SPI 2 and SPI 3 indicators at district level with severe threshold exceeded:
 values aggregated per region and window**



482

483

484 Figure 5: The frequency with which the SPI 2 and SPI 3 indicators exceeded or equaled the severe drought threshold since 1981 is
 485 shown for each zone and window. The counts are first calculated at the district level and then aggregated by zone for window 1 (left)
 486 and window 2 (right). For details on which SPI 2 and SPI 3 indicators correspond to each window, refer to Table 2. The zones are
 487 defined as follows: i) Central zone includes districts from the provinces of Manica, Sofala, Tete, and Zambezia, ii) North zone includes
 488 districts from Nampula, Cabo Delgado, and Niassa, and iii) South zone includes districts from Gaza, Inhambane, Maputo City, and
 489 Maputo Province. Bars are color-coded according to the dominant ENSO phase during the rainy season in Mozambique (red = El
 490 Niño, blue = La Niña, and grey = Neutral). The top 5 years for each window and zone are highlighted.

491

492

494 3.2 Zonal based overview of bias correction

495 Figure 6 presents the percentage of areas per zone, SPI indicator, and forecast month that showed an
496 improved AUROC score after applying bias correction. The primary focus of our evaluation is the AUROC
497 score, as it offers a practical measure of whether bias correction enhances the accuracy of severe drought
498 forecasts, which is crucial for users. The goal of this approach is to identify opportunities for improving
499 forecast accuracy, thereby reducing the risk of misallocated anticipatory action resources due to
500 inaccurate predictions. For a spatial representation, similar results are displayed in a series of maps in
501 Supplementary Material S3.

502

503 Overall, the North zone showed the highest mean percentage of improved forecast areas (38%), followed
504 by the Central and South zones (both at 19%). In the North zone, the forecast month with the highest
505 mean improvement was July (56%), while February had the lowest (20%). For the Central zone, January
506 showed the greatest improvement (26%), while August showed the least (10%). In the South zone, July
507 and August had the highest mean improvement (26%), whereas December and January had the lowest
508 (14%). Across all forecast months, the SPI indicators that demonstrated the greatest skill improvement
509 were SPI ON, SPI DJ, and SPI NDJ for the North zone, SPI JFM for the Central zone, and SPI ON for the South
510 zone. Most of these indicators pertain to the first window of the rainy season in the country.

511

512 Additionally, for all districts and all SPI 2 and SPI 3 indicators across all lead times, 24% demonstrated
513 improved skill (measured by AUROC score) after bias correction compared to the raw forecast. A more
514 detailed overview of the AUROC scores can be found in section 3.3.

515

516

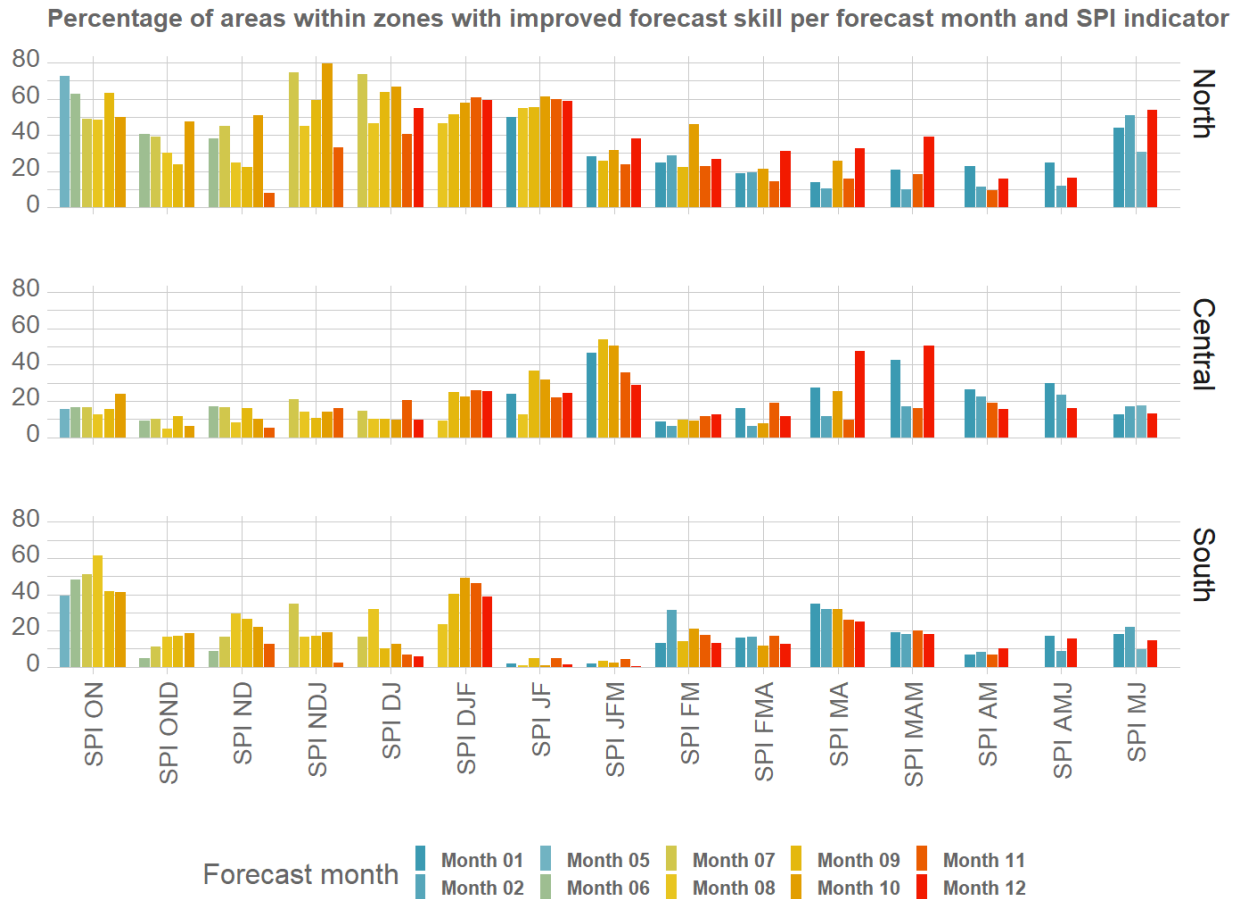


Figure 6: Percentage of zonal areas in which skill has gained using bias correction for different lead times of the forecast used to extract the SPI 2 and SPI 3 indicators.

517
518
519

520

521 3.3 Overview of the maximum AUROC score

522 Figure 7 shows the mean AUROC index per district for predicting severe droughts, combining outcomes
523 from both raw and bias-corrected forecasts across all extracted SPI 2 and SPI 3 periods and lead times. On
524 average, the SPI DJ indicator had the highest AUROC score (0.79), while SPI AM had the lowest (0.63).
525 Severe drought events are generally more predictable during the early to mid-rainy season (average
526 AUROC score of 0.76 for window 1; see Table 2 for indicator details) compared to the mid to late rainy
527 season (average AUROC score of 0.69 for window 2). In particular, the predictability of severe droughts in
528 districts located in the South zone is notably high during window 1 (average AUROC = 0.77), primarily
529 driven by high forecast accuracy in December and January (SPI 2 DJ). In the Central and North zones,
530 severe droughts are most predictable during December to February (average AUROC of 0.78) and
531 November to January (average AUROC of 0.80), respectively.

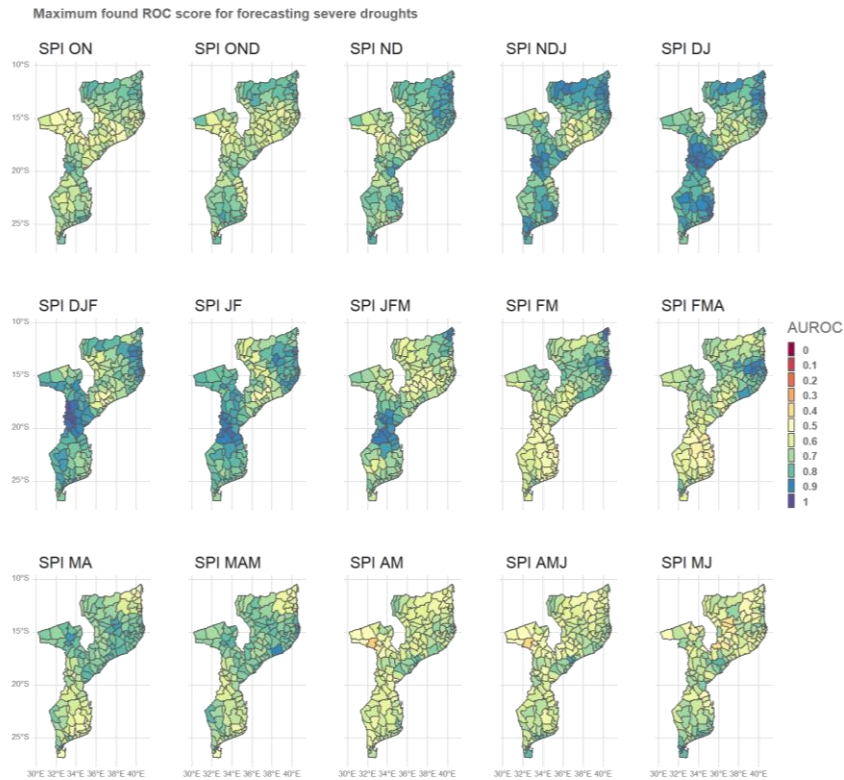
532

533 In Supplementary Material S4, we highlight the lead times that yield the highest forecast skill for severe
534 drought prediction. In the South zone, about 44% of districts achieve the highest AUROC score using the
535 December forecast for SPI DJ. In the Central zone, 55% of districts achieve their best performance using

536 the August forecast for SPI DJF. In the North zone, around 66% of districts see their highest AUROC scores
537 based on the November forecast for SPI NDJ.

538
539 However, it is crucial to note that the implementation of AA requires at least one full month for the "Go!"
540 phase (see Table 1 for criteria). As a result, forecasts released in November, which predict severe droughts
541 between November and January, are not used in operational mode. This means that the "Ready, Set, Go!"
542 trigger system often cannot rely on the most accurate lead times, as they do not allow enough time for
543 action mobilization.

544
545



546
547 Figure 7: Overview of the maximum AUROC score across lead times combining outcomes of both raw and bias corrected forecast.

548
549 After determining whether to use the raw or bias-corrected forecast for a specific lead time, SPI indicator,
550 and district, we move to the most computationally intensive phase of the "Ready, Set, Go!" trigger system.
551 This phase involves testing pairs of triggers for AA, as described in the section "Testing Several Triggers
552 for the Ready, Set, Go! System." The testing is conducted in 1% increments, ranging from 0% to 100%,
553 resulting in 10,201 combinations of candidate triggers per district, forecast month pair, and SPI 2/SPI 3
554 indicator. After testing all combinations and recording their statistical performance, only the best-
555 performing trigger pair for each window is selected for presentation in the next section. The statistical
556 performance of triggers, for the different scenarios, is based on the overall performance using hindcasts
557 from 1993 and 2021 against observed SPI 2 and SPI 3 values within this period.
558

559 All selected trigger pairs must meet the quality criteria outlined in Table 1. To evaluate the value of using
560 mixed forecast information (raw and bias-corrected) with a double-confirmation approach, we expanded
561 the analysis to include additional testing. This extended analysis examines the performance of single
562 versus double triggers and the impact of including or excluding bias correction in the methodology.

563 3.4 Sensitivity Analysis

564 Table 3 presents the average performance of the best triggers for AA during both window 1 and window
565 2, comparing different activation mechanisms. To recap:

- 566 • Scenario 1: Issues an AA advisory based on a single alert using only the raw SPI forecasts from a
567 specific lead time. If the forecast for a specific month, district, and indicator exceeds the assigned
568 probabilistic trigger, an AA advisory is issued and implemented.
- 569 • Scenario 2: Issues an AA advisory based on a single alert, using either raw or bias corrected SPI
570 forecasts, depending on which has higher predictive skill.
- 571 • Scenario 3: Requires double confirmation of drought conditions but uses only raw SPI forecasts.
- 572 • Scenario 4: Represents the operational Ready, Set, & Go! system, which issues an AA advisory
573 based on double confirmation, using a combination of both bias corrected and raw SPI forecasts.

574

575 Overall, scenarios using a double-confirmation approach perform better than those relying on a single
576 drought alert for AA activation.

577

578 Specifically, in the simplest scenario (Scenario 1), 59% of districts in Mozambique would be covered by a
579 General AA trigger, while 42% would be covered by an Emergency trigger (see the section “Apply pre-
580 mapped quality criteria for the triggers’ choice” for definitions of these trigger types). This indicates that
581 raw forecasts alone provide reasonably accurate severe drought predictions for many districts.
582 Incorporating bias correction (Scenario 2) only marginally increases coverage to 61% (General trigger) and
583 43% (Emergency trigger).

584

585 However, applying a double-confirmation approach significantly increases the proportion of districts
586 covered by an AA trigger. In Scenario 3, coverage increases to 73% (General trigger) and 59% (Emergency
587 trigger). Scenario 4, which is the operational system in Mozambique, achieves the highest national AA
588 coverage across all approaches. Additionally, the Ready, Set, & Go! system improves both the hit rate and
589 reduces the false alarm ratio compared to single-alert systems (Scenarios 1 & 2). Furthermore, the Ready,
590 Set, & Go! approach extends the lead time for preparedness activities. While single-alert scenarios
591 provide, on average, 2 months of lead time for AA implementation once the trigger is exceeded, the
592 Ready, Set, & Go! system increases this lead time to nearly 3 months.

593

594

595

596
597
598

Table 3: Sensitivity analysis of different approaches for establishing an AA drought trigger system for the two menu of triggers. Statistics of the different scenarios are based on the average of the best performing SPI 2 or SPI 3 indicator for AA within windows 1 and 2.

		Scenario 1: single drought alert and raw forecast only	Scenario 2: single drought alert including bias corrected forecast	Scenario 3: double confirmation and raw forecast only	Scenario 4: Ready, Set & Go! and including bias corrected forecast
General triggers	Hit Rate	62%	62%	64%	64%
	False Alarm Ratio	21%	21%	17%	16%
	Lead Time for preparedness	2,10	2,00	2,90	2,90
	AA coverage	59%	61%	73%	76%
Emergency triggers	Hit Rate	72%	72%	73%	73%
	False Alarm Ratio	29%	30%	26%	26%
	Lead Time for preparedness	2,10	2,10	3	2,90
	AA coverage	42%	43%	59%	63%

599

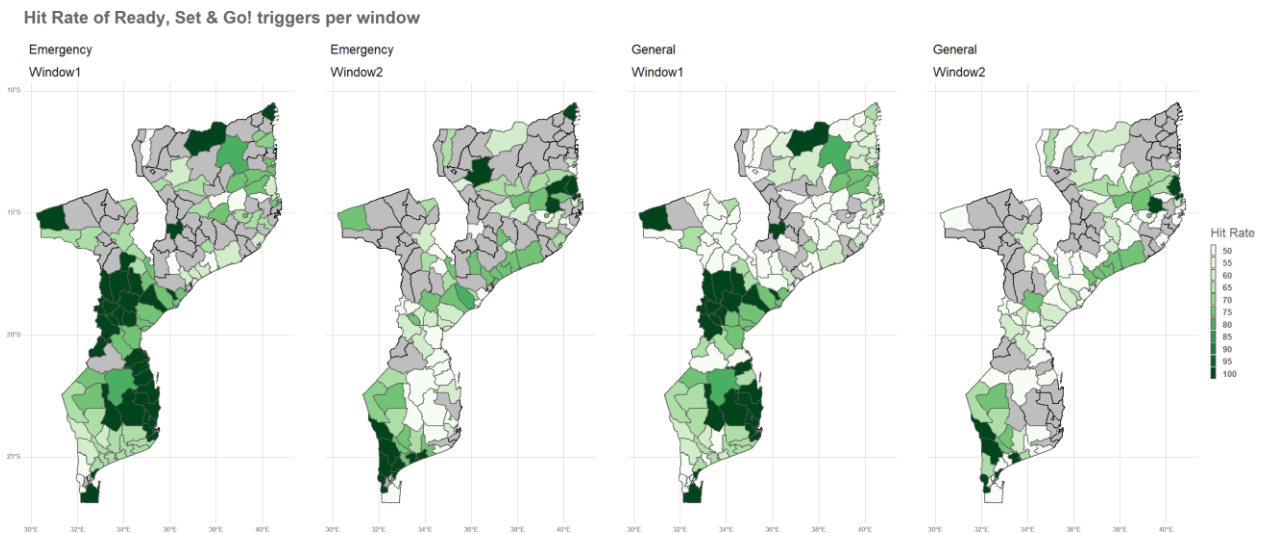
600 3.5 Spatial Overview of Ready, Set & Go! System

601 Figure 8 provides a detailed spatial statistical overview of the performance of the Ready, Set, & Go!
602 triggers, complementing the results for Scenario 4 presented in section 3.4. As noted earlier, severe
603 droughts are predicted with greater skill in window 1 compared to window 2, allowing for AA triggers to
604 be assigned to more districts in window 1. The percentage of districts with a valid AA trigger is as follows:
605 i) 66% for the emergency trigger menu in window 1 and 59% in window 2, and ii) 87% for the general
606 trigger menu in window 1 and 64% in window 2. Notably, every district with an emergency AA trigger also
607 has a general AA trigger, indicating that for most districts, AA triggers can be adjusted annually based on
608 current vulnerability levels. However, in some cases, the general trigger is the only applicable option.

609
610 In terms of trigger performance across windows, the Central zone showed the highest and lowest mean
611 hit rates, with window 1 achieving 74% and window 2 achieving 61%. Across all menus and windows, the
612 emergency menu in window 1 had the highest mean hit rate (77%), while the general menu in window 2
613 had the lowest (61%). This result is expected, as the emergency menu is designed for higher hit rates,
614 particularly given the greater predictability of severe droughts in window 1.

615
616 In addition to the highest drought predictability, the South zone of Mozambique also exhibited the highest
617 total AA coverage, with an average of 86% of districts having an AA trigger. The highest single window and
618 trigger menu coverage was in the South zone under the general menu, with 97% of districts having a
619 trigger. Spatial differences in trigger performance were also observed between neighboring provinces,
620 such as Manica and Tete in window 1 under the general menu. These differences could be driven by

621 varying forecast skill levels. For instance, the AUROC scores for the general trigger in window 1 are 0.82
 622 for Manica and 0.68 for Tete. Factors contributing to these differences could include under- or over-
 623 estimation of rainfall events used to verify forecasts in Mozambique (as noted in a previous study by Toté
 624 et al., 2015), numerical effects from data rescaling, and the resolution of district-level assessments using
 625 CHIRPS and ECMWF forecasts.
 626



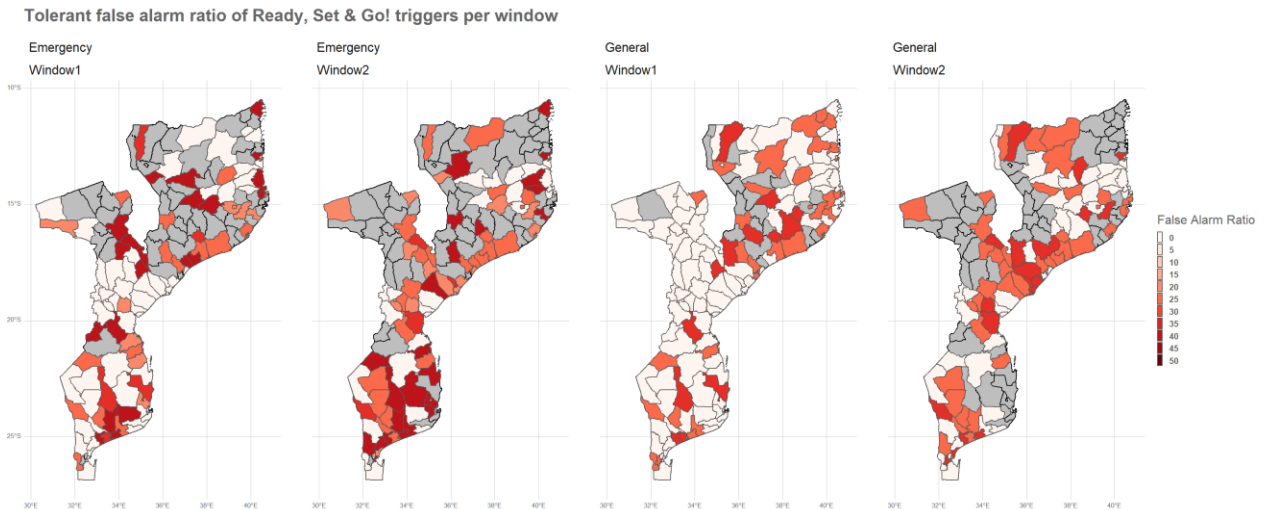
627
 628 Figure 8: Hit rate of the Ready, Set & Go! Trigger system for severe droughts for two trigger menu (emergency and general) and two
 629 windows of intervention (window 1 and window 2). No trigger for the Ready, Set & Go! for severe droughts were found for the districts
 630 in grey.

631
 632 Regarding the average false alarm ratio of the triggers across different windows (Figure 9), the highest
 633 and lowest ratios are observed in the South zone for window 2 (20%) and the Central zone for window 1
 634 (10%), respectively. Across various menus and windows, the emergency menu and window 2 exhibit the
 635 highest false alarm ratio (16%), while the general menu and window 1 have the lowest (10%). This pattern
 636 is expected, as the emergency menu is designed to tolerate a higher false alarm ratio to ensure a higher
 637 hit rate, making it less prone to missing a drought forecast.
 638

639 Supplementary Material S5 details the specific SPI indicators used for AA triggers. For window 1, SPI DJ is
 640 the most commonly selected indicator across all zones. In window 2, different SPIs are chosen per zone:
 641 i) SPI FMA for the North zone, ii) SPI JFM for the Central zone, and iii) SPI DJF for the South zone.
 642

643 Regarding lead times, the earliest “ready” alert for preparedness in window 1 can be issued for a few
 644 districts in the South zone based on the May forecast. However, for most districts in the South zone, the
 645 July forecast is used for preparedness, whereas in the North and Central zones, the September forecast is
 646 most commonly used for the “ready” alert. In window 2, most districts in the South zone use the August
 647 forecast for preparedness, while the North and Central zones typically use the October forecast.
 648

649 It is important to note that regional rainfall climatology significantly influences the choice of intervention
 650 windows and indicators. As a result, districts in the South zone may receive readiness alerts earlier in the
 651 season compared to other areas. This factor is crucial for planning AA activities and allocating geographical
 652 funding.
 653



654
 655 Figure 9: False Alarm ratio of the Ready, Set & Go! Trigger system for severe droughts for two trigger menu (emergency and general)
 656 and two windows of intervention (window 1 and window 2). No trigger for the Ready, Set & Go! for severe droughts were found for the
 657 districts in grey.

658

659 4. DISCUSSION, LIMITATIONS AND NEXT STEPS

660 In this study, we present the methodology behind the operational Ready, Set & Go! trigger system used
 661 by Mozambican governmental institutions and their partners to guide AA activities against droughts. The
 662 system optimizes the use of seasonal forecast information by identifying triggers for AA through a double
 663 confirmation process. This approach combines longer and shorter lead time forecasts to issue more
 664 reliable drought alerts. Our findings indicate that by utilizing both bias corrected and raw ensemble
 665 rainfall forecasts, AA efforts could potentially be scaled up to cover the entire rainy season in, 76% of
 666 Mozambique's district. If focused solely on the first part of the rainy season, where drought predictability
 667 is higher, AA activities could expand to 87% of all districts. This demonstrates that seasonal forecasts can
 668 reliably inform AA months before the onset of severe droughts, meeting the quality criteria established
 669 by multiple institutions. Such scalability indicates strong potential for expanding current AA pilots
 670 nationwide, supporting the ambitious goals of the Maputo Declaration where Southern Africa
 671 governments committed to extending early warning systems across the region (SADC, 2022). Globally,
 672 the Ready, Set & Go! system also aligns with the *Early Warning for All* initiative, which aims to ensure
 673 that every individual worldwide is protected from climate events through early warning systems by 2027
 674 (WMO, 2022). This initiative underscores the need for expanding the climate information portfolio of

675 national meteorological and hydrological services for direct application in disaster risk management.
676 However, there are still limitations and opportunities for improvements , which we discuss in the following
677 sections.

678
679 This study demonstrates that the Ready, Set & Go! Trigger system can effectively issue severe drought
680 alerts using SPI 2 and SPI 3 indicators, which the Technical Working Group in Mozambique has deemed
681 suitable for monitoring and anticipating drought risks in agricultural systems. However, these indicators
682 and thresholds are not flawless in detecting drought damage, as the relationship between drought risk
683 and impact is often location-specific, non-linear, and influenced by non-climatic factors such as
684 vulnerability (Brida et al., 2013; Silva & Matyas, 2014). The ideal method for establishing AA thresholds
685 that reliably detect drought-related losses would involve an historical analysis examining the connection
686 between drought events and socio-economic impacts, such as crop yields, income losses, health
687 outcomes, and food security. Past studies on index-based insurance for the agricultural sector have
688 extensively explored the gap between rainfall measurements and actual agricultural losses, highlighting
689 challenges in accurately capturing real world farmer impacts (Clarke & Dercon, 2009; Clement et al., 2018;
690 Greatrex et al., 2015). Unfortunately, comprehensive, downscaled impact data is largely unavailable,
691 particularly across African countries, limiting further refinement of thresholds and indicators within the
692 system and hindering the ability to solidify links between drought conditions and past impacts. Future
693 efforts should focus on refining these thresholds to strengthen the relationship between physical drought
694 hazards and expected impacts. This could be achieved by utilizing spatially explicit socio-economic
695 datasets, such as the Integrated Food Security Phase Classification indicator from the Famine Early
696 Warning Systems Network, along with data recovery exercises. This would allow users to better
697 understand food security outcomes tied to drought events.

698 Additionally, the Ready, Set & Go! system issues drought alerts based on a multi-month SPI indicator,
699 which can overlook the effects of short but impactful dry spells, poorly distributed rainfall, intense rainfall
700 episodes, or delayed/early cessation of rains. Incorporating additional drought indicators could help
701 better capture these risks, ideally through an exploratory analysis that links specific drought indicators to
702 negative impacts and evaluates their predictability.

703 Two technical aspects related to the extraction of the SPI indicator also requires further improvement.
704 First, more sensitive statistical tests could be used to identify candidate probability distributions for
705 normalizing drought indices. Although this study applies the two-parameter gamma distribution, as
706 recommended by Stagge et al. (2015), a more rigorous assessment of the assumed SPI distributions could
707 be beneficial. Second, the handling of zero precipitation poses challenges, particularly in regions with very
708 low seasonal rainfall. In this system, zero precipitation events are accounted for by assigning SPI values
709 based on their historical occurrence. However, this approach can be problematic when many zero values
710 are present, as SPI requires a mean value of 0 to reflect typical conditions, where half of the years is
711 wetter, and half is drier. While the presence of zero precipitation was rare in this study, further refinement
712 is needed to handle these cases more effectively. Using a method such as the center of probability mass,
713 as suggested by Stagge et al. (2015), could offer a more robust approach to calculating SPI in extremely
714 dry regions.

715

716 The Ready, Set & Go! Trigger system aims to extend AA and reliable early warning information to all
717 districts in Mozambique. Although we have not yet fully achieved this goal using our current technique ,
718 we believe that refining the bias correction methodology will enhance the system’s effectiveness. Bias
719 correction is a critical element in precipitation forecasts, with QM being one of the most commonly
720 applied techniques. In developing AA trigger system, we designed and evaluated a bias correction
721 methodology to improve the accuracy of seasonal forecast in predicting severe droughts. While our
722 methodology has increased forecast for 24% of the predicted SPI at the district level and expanded AA
723 coverage by 4% (as shown in Table 3, comparing scenario 3 to 4), there is still potential to further enhance
724 the bias correction approach. Below, we outline the improvements that can be made.

725

726 Firstly, our method uses an ENSO-informed quantile mapping transfer function to correct the SPI forecast
727 based on the SPI reference value of the pixel under investigation and its nine neighboring pixels
728 conditioned on the state of ENSO. This process ensures that the bias correction accounts for variations in
729 the SPI quantities according to the climatology of different ENSO phases, effectively capturing relevant
730 global processes (Manzanas & Gutiérrez, 2019; Maraun et al., 2017). In practice, this involves splitting SPI
731 time series, derived from both CHIRPS and ECMWF ensemble forecasts, into Neutral, La Niña and El Niño
732 years depending on the ENSO phase (detailed in Supplementary Material S1). However, in some regions
733 of Mozambique, such as part of Tete, the ENSO-rainfall signal is weak, particularly during October to
734 December (WFP, 2018). Therefore, relying solely on an ENSO-based approach may not be the ideal in
735 these areas. Other climate variability modes, such as the Indian Ocean Dipole, are also known to influence
736 annual rainfall variability in the Mozambique (Ficchi et al., 2021; Harp et al., 2021; Ogwang BA, Ongoma
737 V, Shilenje ZW, Ramotubei TS, Letuma M, 2021). This suggests a need to investigate the suitability of
738 incorporating additional teleconnections modes into the bias correction process.

739

740 Second, since extreme droughts generally affect broad areas rather than single locations (Eskridge et al.,
741 1997; Liu et al., 2021), our bias correction methodology accounts for the spatial dependence of SPI. To
742 bias correct a single grid point of the SPI ensemble forecast, we incorporate data from multiple grid points
743 (the target grid point and its nine neighbors) from the reference SPI dataset to build the transfer function.
744 Previous research has shown that addressing spatial dependence reduces bias in climate model outputs
745 (Cannon, 2018; Nahar et al., 2018). To avoid overfitting, we use a leave-one-year-out cross-validation
746 scheme, excluding the year being bias corrected from the transfer function. For the spatial dependence
747 setup, we tested two k values (4 and 9), ultimately selecting 9 based on improved spatial homogeneity of
748 AUROC scores. However, this approach could benefit from further optimization by assessing the k value
749 that yields the highest AUROC scores for specific locations.

750

751 Third, improvements in bias correction may be achieved by exploring emerging methodologies such as
752 Machine Learning (ML). Recent studies indicate that ML has the potential to outperform traditional
753 techniques like QM (e.g., Yoshikane & Yoshimura, 2023; Zarei et al., 2021). Lastly, our initial internal tests
754 showed significant improvements in drought predictability by creating a transfer function that directly
755 links SPI forecasts to SPI observations, rather than taking the traditional approach of bias correcting daily
756 or monthly raw rainfall forecasts before converting them into SPI values. This direct approach has led to

757 both statistical and practical gains, as it allows the system to focus directly on drought detection. If the
758 system evolves to include additional rainfall-based indicators, such as dry spells or the start/cessation of
759 rains, a method that directly bias corrects raw forecasts could offer operational advantages, as it can be
760 widely applied to generate additional indicators.

761
762 We also highlight the potential to scale up AA by utilizing rainfall seasonal forecasts from the ECWMF. In
763 our approach, the seasonal forecast is downscaled from 1 degree to 0.25 degrees using bilinear
764 interpolation, which allows us to assess forecasting skill at the district level. Extracting drought alerts at
765 the district level is crucial to align with the geographical targeting of AA interventions. However, further
766 investigation into other downscaling techniques, such as ML, could be beneficial, as ML has been shown
767 to enhance forecast skill (Jin et al., 2023). ECMWF was initially selected as our primary source of
768 forecasting information due to its superior skill in predicting precipitation over the African continent
769 compared to other centers (Gebrechorkos et al., 2022). Nevertheless, future studies may benefit from
770 shifting from a single-model approach to a Multi-Model Ensemble (MME) strategy. MME integrates
771 independent models from various forecasting centers of information, which helps mitigate model errors
772 and can enhance the reliability of seasonal outlooks (Doblas-Reyes et al., 2010; Gebrechorkos et al., 2022;
773 Rozante et al., 2014)

774
775 We demonstrate that the Ready, Set & Go! system improves the accuracy of AA advisories, resulting in a
776 higher hit rate and a lower false alarm ratio compared to a system that relies on a single alert for AA
777 advisories. Additionally, we observe that this system extends the lead time for preparedness activities,
778 allowing for the scaling up of AA efforts against severe droughts during the first window of the rainy
779 season, covering 87% of districts in Mozambique. However, since AA triggers are identified and optimized
780 at the district level, the system is prone to issuing advisories for individual districts, even though past
781 severe droughts have often had broader impacts, including widespread socio-economic consequences
782 (Baez et al., 2020). This discrepancy may occur because the system uses different lead times for
783 forecasting information across districts within the same province or because triggers for different
784 implementation windows within a province are based on varying SPI indicators. An example of this can be
785 seen in southern Mozambique (refer to Supplementary Material S5). Despite these statistical gains,
786 optimizing AA triggers at the district level needs to be contextualized for practical decision-making,
787 particularly for large-scale operations and the distribution and management of funding. Therefore, while
788 district-level optimization may be effective statistically, it may not always be the most appropriate
789 approach for AA planning, especially when scaling up AA across the entire country. One potential solution
790 to avoid asynchrony in AA triggers is to refine the selection of indicators and lead times by evaluating their
791 performance across the majority of districts within a province, ensuring more synchronized and
792 coordinated AA efforts.

793
794 We also demonstrate that the triggers for the Ready, Set & Go! system can be adjusted based on
795 vulnerability information, adding an important nuance to AA operations (Baez et al., 2020). However,
796 measuring vulnerability is a complex task that often requires frequent updates, location-specific data, and
797 further disaggregation by age and gender (Chaves-Gonzalez et al., 2022). In Mozambique, the Technical
798 Secretariat for Food Security and Nutrition (SETSAN) is responsible for providing such information. AA

799 operations would greatly benefit if this data were made available in a timely manner, ideally before the
800 start of the AA season. Unfortunately, this is not always the case. More research is needed to understand
801 vulnerability trends and their relationship to climate hazards (Baez et al., 2020; Hallegatte et al., 2016). As
802 the system expands, collecting timely vulnerability data may become increasingly challenging. Therefore,
803 a systematic, rapid, yet robust methodology for vulnerability analysis is essential. We have also observed
804 a lower percentage of districts covered by AA when emergency triggers—modulated by vulnerability—
805 are used. These emergency triggers inherently allow for a higher rate of false alarms and focus on "no-
806 regret" actions (Chaves-Gonzalez et al., 2022) while increasing the probability of detection. This approach
807 aims to maximize the number of extreme droughts anticipated by AA interventions and provide a safety
808 net for areas with high vulnerability. However, the current criteria for identifying emergency triggers are
809 not achieving higher coverage compared to general triggers. Revisiting these criteria (see Table 1) through
810 a statistical optimization process may help enhance the system's effectiveness.

811
812 As previously mentioned, the Ready, Set & Go! system is currently being piloted in 11 districts across
813 Mozambique, with plans to scale up AA operations in 2024. Due the 2023-24 El Niño, several AA advisories
814 have already been issued to districts in the Gaza, Sofala, and Tete provinces, marking the system's first
815 operational deployment during the 2023-24 rainy season. While humanitarian and governmental
816 organizations have substantial experience in responding to hazards after they occur, most monitoring and
817 evaluation (M&E) efforts have focused on the effects of emergency responses post-crisis. There is limited
818 evidence on the benefits of AA, particularly regarding drought interventions partially given the small
819 number of pilot interventions to date as well as with challenges faced by studies on benefit
820 estimations/modelling. As the evidence base for value for money begins to form, WFP's AA programs are
821 showing potential as a sustainable way to support climate-vulnerable governments with limited resources
822 (WFP, 2023a). In Kenya, drought-related AA could save up to US\$20 billion over 20 years, even with false
823 alarms costing significantly less than a late response. In Ethiopia, Kenya, and Somalia, AA could save
824 US\$1.6 billion over 15 years by mitigating drought impacts before price spikes and negative coping
825 strategies. In Nepal, AA reduced damage to vulnerable populations by 75% and cuts asset losses by 50%,
826 saving US\$34 for every dollar invested and reducing long-term recovery costs. In Zimbabwe, AA reached
827 32,500 people before drought impacts, with 97% of farmers benefiting from climate information and 80%
828 adapting their practices, leading to higher resilience compared to a control group.

829
830 Given that AA represents an innovative approach and a relatively new concept in risk management, it is
831 crucial to establish a robust M&E system to evaluate the effectiveness of AA interventions. This system
832 will provide valuable insights into what has worked well in practice and highlight areas for improvement
833 in future operations. Ultimately, a well-designed M&E process will help determine whether AA
834 interventions are effectively reducing or mitigating the impacts of droughts on affected populations (Gros
835 et al., 2021)

836

837 5. CONCLUSIONS AND RECOMMENDATIONS

838 In this article, we introduced and benchmarked the “Ready, Set & Go!” system, which is being piloted in
839 Mozambique to trigger anticipatory action against severe droughts. This system is designed to implement
840 measures that mitigate the impacts of rainfall deficits during the critical period between forecasting and
841 the onset of drought. Following the recent adoption of the SADC Maputo Declaration by its member
842 states, there is a need to evaluate the system's opportunities and limitations for expanding drought AA
843 coverage to all districts in Mozambique. Our study findings include:

- 844
845 • Potential for Expansion: The Ready, Set & Go! system could potentially scale AA activities to 76%
846 of Mozambican districts. Additionally, 63% of these districts could adopt an alternative trigger
847 system tailored to vulnerability levels. This feature allows the system to proactively address
848 potential vulnerabilities for the upcoming season. If only the first window of the rainy season is
849 targeted, coverage could increase to 87%.
- 850 • Impact of Bias Correction: The bias correction methodology used in the Ready, Set & Go! system
851 enhances forecasting skill for 24% of all forecasted SPI indicators at the district level. This
852 improvement slightly raises AA coverage from 73% to 76% for the general menu, and from 59%
853 to 63% for the emergency menu. This means bias correction can extend operational AA coverage
854 to about six additional districts, representing a slight improvement but also enhancing the
855 potential for life-saving AA.
- 856 • Increased Hit Rate and Lead Time: The Ready, Set & Go! system improves both the hit rate and
857 lead time for AA compared to three alternative triggering approaches. The highest mean hit rate
858 across different windows was observed in the Central Zone within window 1 (74%). SPI DJ is the
859 most commonly used indicator for AA in window 1. The earliest “ready” alert for preparedness
860 can be issued for a few districts in the South zone based on the May forecast.
- 861 • Reduced False Alarm Ratio: The Ready, Set & Go! system achieves a lower false alarm ratio
862 compared to the three alternative approaches. The mean lowest average false alarm ratio is found
863 in the Central Zone for window 1 (10%). Among different menus and windows, the mean highest
864 false alarm ratio is 21% for the emergency menu in window 2, while the mean lowest is 10% for
865 the general menu in window 1.

866
867 We observed that the piloted drought EWS has significant potential for scaling up AA across Mozambique,
868 aligning with the goals of the Maputo Declaration and the Early Warning for All initiative to provide climate
869 event coverage and protection to all citizens by 2027. However, several next steps could further enhance
870 the effectiveness of the EWS:

871 872 Enhancing Bias Correction Methodology

- 873 • Explore Additional Climate Indices: Incorporate more indices related to climate variability to
874 refine the transfer function.
- 875 • Optimize Nearest Neighbors: Fine-tune the number of nearest neighbors used in bias correction.
- 876 • Investigate Emerging Techniques: Explore advanced methods such as Machine Learning to
877 improve accuracy.

878

879 Improving Forecast Resolution

- 880 • Explore Downscaling Techniques: Investigate alternative downscaling methods to enhance the
- 881 resolution of seasonal forecasts.
- 882 • Consider Multi-Model Ensemble Approaches: Evaluate whether combining multiple models could
- 883 improve the reliability of seasonal outlooks.

884

885 Strengthening Impact Links

- 886 • Connect Thresholds to Socio-Economic Impacts: Enhance understanding of the socio-economic
- 887 consequences of droughts to better plan and target AA activities.
- 888 • Incorporate Additional Indicators: Include other relevant drought indicators, such as the onset of
- 889 rains and rainfall cessation, to provide a more comprehensive assessment.

890

891 Contextualizing Trigger Optimization

- 892 • Refine Triggers for Practical Decision-Making: Consider the impact of optimizing triggers at the
- 893 district level, which may lead to asynchrony in AA activations among neighboring districts. Select
- 894 SPI 2 or SPI 3 indicators and lead times based on their performance across most districts within a
- 895 province.

896

897 Investing in Monitoring and Evaluation

- 898 • Support Ongoing Pilots: Invest in monitoring, evaluation, and learning to inform future expansion
- 899 of the anticipatory approach and maximize the impact of AA activities.

900

901 These steps may help to maximize the effectiveness and coverage of the EWS, ensuring that AA efforts

902 are timely, more accurate and well-targeted.

903

904 COMPETING INTERESTS

905

906 The contact author has declared that none of the authors has any competing interests.

907

908

909 REFERENCES

- 910 Anticipation Hub. (2024). *Anticipatory action in the world*. <https://www.anticipation->
911 [hub.org/experience/global-map](https://www.anticipation-hub.org/experience/global-map)
- 912 Araneda-Cabrera, R. J., Bermudez, M., & Puertas, J. (2021). Revealing the spatio-temporal characteristics
913 of drought in Mozambique and their relationship with large-scale climate variability. *Journal of*
914 *Hydrology: Regional Studies*, 38, 100938. <https://doi.org/10.1016/j.ejrh.2021.100938>
- 915 Ashok, K., Guan, Z., & Yamagata, T. (2001). Impact of the Indian Ocean dipole on the relationship
916 between the Indian monsoon rainfall and ENSO. *Geophysical Research Letters*, 28(23), 4499–4502.
917 <https://doi.org/10.1029/2001GL013294>
- 918 Baez, J. E., Caruso, G., & Niu, C. (2019). Extreme Weather and Poverty Risk: Evidence from Multiple
919 Shocks in Mozambique. *Economics of Disasters and Climate Change 2019 4:1*, 4(1), 103–127.
920 <https://doi.org/10.1007/S41885-019-00049-9>
- 921 Baez, J. E., Caruso, G., & Niu, C. (2020). Extreme Weather and Poverty Risk: Evidence from Multiple
922 Shocks in Mozambique. *Economics of Disasters and Climate Change*, 4(1), 103–127.
923 <https://doi.org/10.1007/s41885-019-00049-9>
- 924 Behera, S. K., & Yamagata, T. (2001). Subtropical SST dipole events in the southern Indian Ocean.
925 *Geophysical Research Letters*, 28(2), 327–330. <https://doi.org/10.1029/2000GL011451>
- 926 Blamey, R. C., Kolusu, S. R., Mahlalela, P., Todd, M. C., & Reason, C. J. C. (2018). The role of regional
927 circulation features in regulating El Niño climate impacts over southern Africa: A comparison of the
928 2015/2016 drought with previous events. *International Journal of Climatology*, 38(11), 4276–4295.
929 <https://doi.org/10.1002/joc.5668>
- 930 Brida, A. B., Owiyo, T., & Sokona, Y. (2013). Loss and damage from the double blow of flood and drought
931 in Mozambique. *International Journal of Global Warming*, 5(4), 514.
932 <https://doi.org/10.1504/IJGW.2013.057291>
- 933 Cannon, A. J. (2018). Multivariate quantile mapping bias correction: an N-dimensional probability
934 density function transform for climate model simulations of multiple variables. *Climate Dynamics*,
935 50(1–2), 31–49. <https://doi.org/10.1007/s00382-017-3580-6>
- 936 Chaves-Gonzalez, J., Milano, L., Omtzigt, D.-J., Pfister, D., Poirier, J., Pople, A., Wittig, J., & Zommers, Z.
937 (2022). Anticipatory action: Lessons for the future. *Frontiers in Climate*, 4.
938 <https://doi.org/10.3389/fclim.2022.932336>
- 939 Clarke, D., & Dercon, S. (2009). Insurance, credit and safety nets for the poor in a world of risk. *Financ.*
940 *Overcoming Econ. Insecur*, 85.
- 941 Clement, K. Y., Wouter Botzen, W. J., Brouwer, R., & Aerts, J. C. J. H. (2018). A global review of the
942 impact of basis risk on the functioning of and demand for index insurance. *International Journal of*
943 *Disaster Risk Reduction*, 28, 845–853. <https://doi.org/10.1016/j.ijdrr.2018.01.001>
- 944 De Ruiter, M. C., Couasnon, A., van den Homberg, M. J. C., Daniell, J. E., Gill, J. C., & Ward, P. J. (2020).
945 Why we can no longer ignore consecutive disasters. *Earth's Future*, 8(3), e2019EF001425.
- 946 Doblas-Reyes, F. J., Déqué, M., & Pielieuvre, J.-P. (2010). Multi-model spread and probabilistic seasonal
947 forecasts in PROVOST. *Quarterly Journal of the Royal Meteorological Society*, 126(567), 2069–2087.
948 <https://doi.org/10.1002/qj.49712656705>
- 949 ECHO. (2021). *Echo Flash*. <https://ecrcportal.jrc.ec.europa.eu/ECHO-Products/Echo-Flash#/daily-flash->
950 [archive/4117](https://ecrcportal.jrc.ec.europa.eu/ECHO-Products/Echo-Flash#/daily-flash-archive/4117)
- 951 Eskridge, R. E., Ku, J. Y., Rao, S. T., Porter, P. S., & Zurbenko, I. G. (1997). Separating Different Scales of
952 Motion in Time Series of Meteorological Variables. *Bulletin of the American Meteorological Society*,
953 78(7), 1473–1483. [https://doi.org/10.1175/1520-0477\(1997\)078<1473:SDSOMI>2.0.CO;2](https://doi.org/10.1175/1520-0477(1997)078<1473:SDSOMI>2.0.CO;2)
- 954 Fawcett, T. (2006). An introduction to ROC analysis. *Pattern Recognition Letters*, 27(8), 861–874.
955 <https://doi.org/10.1016/j.patrec.2005.10.010>

956 Ficchi, A., Cloke, H., Neves, C., Woolnough, S., Coughlan de Perez, E., Zsoter, E., Pinto, I., Meque, A., &
957 Stephens, E. (2021). Beyond El Niño: Unsung climate modes drive African floods. *Weather and*
958 *Climate Extremes*, 33, 100345. <https://doi.org/10.1016/j.wace.2021.100345>

959 Funk, C., Peterson, P., Landsfeld, M., Pedreros, D., Verdin, J., Shukla, S., Husak, G., Rowland, J., Harrison,
960 L., Hoell, A., & Michaelsen, J. (2015). The climate hazards infrared precipitation with stations - A
961 new environmental record for monitoring extremes. *Scientific Data*.
962 <https://doi.org/10.1038/sdata.2015.66>

963 Gebrechorkos, S. H., Pan, M., Beck, H. E., & Sheffield, J. (2022). Performance of State-of-the-Art C3S
964 European Seasonal Climate Forecast Models for Mean and Extreme Precipitation Over Africa.
965 *Water Resources Research*, 58(3). <https://doi.org/10.1029/2021WR031480>

966 Greatrex, H., Hansen, J., Garvin, S., Diro, R., Le Guen, M., Blakeley, S., Rao, K., & Osgood, D. (2015).
967 Scaling up index insurance for smallholder farmers: Recent evidence and insights. *CCAFS Report*.

968 Gros, C., Heinrich, D., Kazis, P., Merola, S., & others. (2021). *Monitoring and evaluation of anticipatory*
969 *actions for fast and slow-onset hazards: Guidance and tools for Forecast-based Financing*.

970 Guimarães Nobre, G., Pasqui, M., Quaresima, S., Pieretto, S., & Lemos Pereira Bonifácio, R. M. (2023).
971 Forecasting, thresholds, and triggers: Towards developing a Forecast-based Financing system for
972 droughts in Mozambique. *Climate Services*, 30, 100344.
973 <https://doi.org/10.1016/j.cliser.2023.100344>

974 Hallegatte, S., Bangalore, M., Bonzanigo, L., Fay, M., Kane, T., Narloch, U., Rozenberg, J., Treguer, D., &
975 Vogt-Schilb, A. (2016). *Shock Waves: Managing the Impacts of Climate Change on Poverty*.
976 Washington, DC: World Bank. <https://doi.org/10.1596/978-1-4648-0673-5>

977 Harp, R. D., Colborn, J. M., Candrinho, B., Colborn, K. L., Zhang, L., & Karnauskas, K. B. (2021).
978 Interannual Climate Variability and Malaria in Mozambique. *GeoHealth*, 5(2).
979 <https://doi.org/10.1029/2020GH000322>

980 Hart, N. C. G., Reason, C. J. C., & Fauchereau, N. (2010). Tropical–Extratropical Interactions over
981 Southern Africa: Three Cases of Heavy Summer Season Rainfall. *Monthly Weather Review*, 138(7),
982 2608–2623. <https://doi.org/10.1175/2010MWR3070.1>

983 Jin, H., Jiang, W., Chen, M., Li, M., Bakar, K. S., & Shao, Q. (2023). Downscaling long lead time daily
984 rainfall ensemble forecasts through deep learning. *Stochastic Environmental Research and Risk*
985 *Assessment*, 37(8), 3185–3203. <https://doi.org/10.1007/s00477-023-02444-x>

986 Liu, Z., Xie, Y., Cheng, L., Lin, K., Tu, X., & Chen, X. (2021). Stability of spatial dependence structure of
987 extreme precipitation and the concurrent risk over a nested basin. *Journal of Hydrology*, 602,
988 126766. <https://doi.org/10.1016/j.jhydrol.2021.126766>

989 Lloyd-Hughes, B., & Saunders, M. A. (2002). A drought climatology for Europe. *International Journal of*
990 *Climatology*, 22(13), 1571–1592. <https://doi.org/10.1002/JOC.846>

991 Lopez, A., Coughlan de Perez, E., Bazo, J., Suarez, P., van den Hurk, B., & van Aalst, M. (2018). Bridging
992 forecast verification and humanitarian decisions: A valuation approach for setting up action-
993 oriented early warnings. *Weather and Climate Extremes*, April 2016, 1–8.
994 <https://doi.org/10.1016/j.wace.2018.03.006>

995 Lyon, B., & Mason, S. J. (2007). The 1997–98 Summer Rainfall Season in Southern Africa. Part I:
996 Observations. *Journal of Climate*, 20(20), 5134–5148. <https://doi.org/10.1175/JCLI4225.1>

997 Manatsa, D., Matarira, C. H., & Mukwada, G. (2011). Relative impacts of ENSO and Indian Ocean
998 dipole/zonal mode on east SADC rainfall. *International Journal of Climatology*, 31(4), 558–577.
999 <https://doi.org/10.1002/joc.2086>

1000 Manhique, A. J., Reason, C. J. C., Silinto, B., Zucula, J., Raiva, I., Congolo, F., & Mavume, A. F. (2015).
1001 Extreme rainfall and floods in southern Africa in January 2013 and associated circulation patterns.
1002 *Natural Hazards*, 77(2), 679–691. <https://doi.org/10.1007/s11069-015-1616-y>

1003 Manhique, Atanásio João, Guirruço, I. A., Nhantumbo, B. J., & Mavume, A. F. (2021). Seasonal to

1004 Interannual Variability of Vertical Wind Shear and Its Relationship with Tropical Cyclogenesis in the
1005 Mozambique Channel. *Atmosphere*, 12(6), 739. <https://doi.org/10.3390/atmos12060739>
1006 Manzanas, R., & Gutiérrez, J. M. (2019). Process-conditioned bias correction for seasonal forecasting: a
1007 case-study with ENSO in Peru. *Climate Dynamics*, 52(3), 1673–1683.
1008 <https://doi.org/10.1007/s00382-018-4226-z>
1009 Maraun, D., Shepherd, T. G., Widmann, M., Zappa, G., Walton, D., Gutiérrez, J. M., Hagemann, S.,
1010 Richter, I., Soares, P. M. M., Hall, A., & Mearns, L. O. (2017). Towards process-informed bias
1011 correction of climate change simulations. *Nature Climate Change*, 7(11), 764–773.
1012 <https://doi.org/10.1038/nclimate3418>
1013 Mawren, D., Hermes, J., & Reason, C. J. C. (2020). Exceptional Tropical Cyclone Kenneth in the Far
1014 Northern Mozambique Channel and Ocean Eddy Influences. *Geophysical Research Letters*, 47(16).
1015 <https://doi.org/10.1029/2020GL088715>
1016 Nahar, J., Johnson, F., & Sharma, A. (2018). Addressing Spatial Dependence Bias in Climate Model
1017 Simulations—An Independent Component Analysis Approach. *Water Resources Research*, 54(2),
1018 827–841. <https://doi.org/10.1002/2017WR021293>
1019 National Center for Atmospheric Research Staff. (2014). *No The Climate Data Guide: Regridding*
1020 *Overview*. <https://climatedataguide.ucar.edu/climate-tools/regridding-overview>
1021 OCHA. (2017). *Report on the RIASCO Action Plan for the El Niño - Induced Drought in Southern Africa*
1022 *2016/2017*. [https://reliefweb.int/report/world/report-riasco-action-plan-el-ni-o-induced-drought-](https://reliefweb.int/report/world/report-riasco-action-plan-el-ni-o-induced-drought-southern-africa-20162017)
1023 [southern-africa-20162017](https://reliefweb.int/report/world/report-riasco-action-plan-el-ni-o-induced-drought-southern-africa-20162017)
1024 Ogwang BA, Ongoma V, Shilenje ZW, Ramotubei TS, Letuma M, N. J. (2021). Influence of Indian Ocean
1025 dipole on rainfall variability and extremes over southern Africa. *MAUSAM*, 71(4), 637–648.
1026 <https://doi.org/10.54302/mausam.v71i4.50>
1027 Rapolaki, R. S., Blamey, R. C., Hermes, J. C., & Reason, C. J. C. (2019). A classification of synoptic weather
1028 patterns linked to extreme rainfall over the Limpopo River Basin in southern Africa. *Climate*
1029 *Dynamics*, 53(3–4), 2265–2279. <https://doi.org/10.1007/s00382-019-04829-7>
1030 Ratri, D. N., Whan, K., & Schmeits, M. (2019). A Comparative Verification of Raw and Bias-Corrected
1031 ECMWF Seasonal Ensemble Precipitation Reforecasts in Java (Indonesia). *Journal of Applied*
1032 *Meteorology and Climatology*, 58(8), 1709–1723. <https://doi.org/10.1175/JAMC-D-18-0210.1>
1033 Reason, C. J. C., & Keibel, A. (2004). Tropical cyclone Eline and its unusual penetration and impacts over
1034 the southern African mainland. *Weather and Forecasting*, 19(5), 789–805.
1035 Richard, Y., Fauchereau, N., Pocard, I., Rouault, M., & Trzaska, S. (2001). 20th century droughts in
1036 Southern Africa: Spatial and temporal variability, teleconnections with oceanic and atmospheric
1037 conditions. *International Journal of Climatology*, 21(7), 873–885. <https://doi.org/10.1002/joc.656>
1038 Rozante, J. R., Moreira, D. S., Godoy, R. C. M., & Fernandes, A. A. (2014). Multi-model ensemble:
1039 technique and validation. *Geoscientific Model Development*, 7(5), 2333–2343.
1040 <https://doi.org/10.5194/gmd-7-2333-2014>
1041 SADC. (2022). *Maputo Declaration on the Commitment by SADC to enhance Early Warning and Early*
1042 *Action in the Region*. [https://au.int/sites/default/files/pressreleases/42156-other-](https://au.int/sites/default/files/pressreleases/42156-other-Maputo_Declaration_Final_AUC_11_Sept-2022.pdf)
1043 [Maputo_Declaration_Final_AUC_11_Sept-2022.pdf](https://au.int/sites/default/files/pressreleases/42156-other-Maputo_Declaration_Final_AUC_11_Sept-2022.pdf)
1044 Saji, N. H., Goswami, B. N., Vinayachandran, P. N., & Yamagata, T. (1999). A dipole mode in the tropical
1045 Indian Ocean. *Nature*, 401(6751), 360–363. <https://doi.org/10.1038/43854>
1046 Silva, J. A., & Matyas, C. J. (2014). Relating Rainfall Patterns to Agricultural Income: Implications for Rural
1047 Development in Mozambique. *Weather, Climate, and Society*, 6(2), 218–237.
1048 <https://doi.org/10.1175/WCAS-D-13-00012.1>
1049 Stagge, J. H., Tallaksen, L. M., Gudmundsson, L., Van Loon, A. F., & Stahl, K. (2015). Candidate
1050 Distributions for Climatological Drought Indices (SPI and SPEI). *International Journal of Climatology*,
1051 35(13), 4027–4040. <https://doi.org/10.1002/joc.4267>

1052 Svoboda, M., Hayes, M., Wood, D. A., & others. (2012). *Standardized precipitation index user guide*.
1053 Trambauer, P., Werner, M., Winsemius, H. C., Maskey, S., Dutra, E., & Uhlenbrook, S. (2015).
1054 Hydrological drought forecasting and skill assessment for the Limpopo River basin, southern Africa.
1055 *Hydrology and Earth System Sciences*, 19(4), 1695–1711.
1056 Weingärtner, L., Pforr, T., & Wilkinson, E. (2020). *The evidence base on Anticipatory Action*.
1057 WFP. (2016). *WFP Regional Bureau for Southern Africa SPECIAL OPERATION 200993*.
1058 <https://documents.wfp.org/stellent/groups/internal/documents/projects/wfp285532.pdf>
1059 WFP. (2018). *MOZAMBIQUE: A Climate Analysis*. <https://doi.org/10.54302/mausam.v71i4.50>
1060 WFP. (2023a). *Anticipatory Action for Climate Shocks*. Success Stories.
1061 <https://www.wfp.org/anticipatory-actions>
1062 WFP. (2023b). *Building systems to anticipate drought in Mozambique*.
1063 [https://reliefweb.int/report/mozambique/anticipatory-action-building-systems-anticipate-](https://reliefweb.int/report/mozambique/anticipatory-action-building-systems-anticipate-drought-mozambique-impact-assessment-wfps-capacity-strengthening-interventions-national-systems-september-2023)
1064 [drought-mozambique-impact-assessment-wfps-capacity-strengthening-interventions-national-](https://reliefweb.int/report/mozambique/anticipatory-action-building-systems-anticipate-drought-mozambique-impact-assessment-wfps-capacity-strengthening-interventions-national-systems-september-2023)
1065 [systems-september-2023](https://reliefweb.int/report/mozambique/anticipatory-action-building-systems-anticipate-drought-mozambique-impact-assessment-wfps-capacity-strengthening-interventions-national-systems-september-2023)
1066 Winsemius, H. C., Dutra, E., Engelbrecht, F. A., Archer Van Garderen, E., Wetterhall, F., Pappenberger, F.,
1067 & Werner, M. G. F. (2014). The potential value of seasonal forecasts in a changing climate in
1068 southern Africa. *Hydrology and Earth System Sciences*, 18(4), 1525–1538.
1069 <https://doi.org/10.5194/hess-18-1525-2014>
1070 WMO. (2022). *Early Warnings For All: The UN Global Early Warning Initiative for the Implementation of*
1071 *Climate Adaptation*. <https://library.wmo.int/records/item/58209-early-warnings-for-all>
1072 World Bank. (2018). *Mozambique food market monitoring and resilient agriculture planning. Policy*
1073 *Report, 645 Washington D.C.*
1074 Yoshikane, T., & Yoshimura, K. (2023). A downscaling and bias correction method for climate model
1075 ensemble simulations of local-scale hourly precipitation. *Scientific Reports*, 13(1), 9412.
1076 <https://doi.org/10.1038/s41598-023-36489-3>
1077 Zarei, M., Najarchi, M., & Mastouri, R. (2021). Bias correction of global ensemble precipitation forecasts
1078 by Random Forest method. *Earth Science Informatics*, 14(2), 677–689.
1079 <https://doi.org/10.1007/s12145-021-00577-7>
1080